

# Rothamsted Repository Download

## A - Papers appearing in refereed journals

Neal, A. L., McLaren, T., Campolino, M. L., Hughes, D. J., Coelho, A. M., De Paula Lana, U. G., Gomes, E. A. and De Sousa, S. M. 2020. Crop Type Exerts Greater Influence Upon Rhizosphere Phosphohydrolase Gene Abundance and Phylogenetic Diversity than Phosphorus Fertilization. *FEMS Microbiology Ecology*. 97 (4), p. fiab033.  
<https://doi.org/10.1093/femsec/fiab033>

The publisher's version can be accessed at:

- <https://doi.org/10.1093/femsec/fiab033>

The output can be accessed at: <https://repository.rothamsted.ac.uk/item/97840/crop-type-exerts-greater-influence-upon-rhizosphere-phosphohydrolase-gene-abundance-and-phylogenetic-diversity-than-phosphorus-fertilization>.

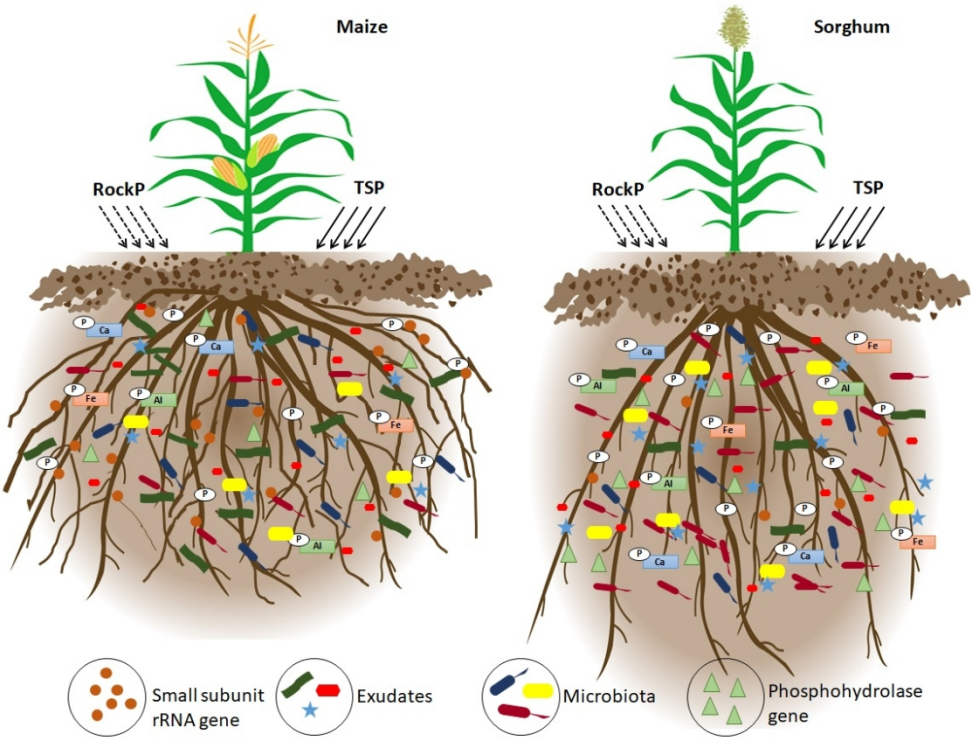
© 20 February 2021, Please contact [library@rothamsted.ac.uk](mailto:library@rothamsted.ac.uk) for copyright queries.

<http://mc.manuscriptcentral.com/fems>

**Crop Type Exerts Greater Influence Upon Rhizosphere  
Phosphohydrolase Gene Abundance and Phylogenetic  
Diversity than Phosphorus Fertilization**

Journal:	<i>FEMS Microbiology Ecology</i>
Manuscript ID	Draft
Manuscript Type:	Research article
Date Submitted by the Author:	n/a
Complete List of Authors:	<p>Neal, Andrew; Rothamsted Research, Department of Sustainable Agriculture Science</p> <p>McLaren, Timothy; ETH Zürich, Department of Environmental Systems Science</p> <p>Lourenço Campolino, Mariana; Empresa Brasileira de Pesquisa Agropecuaria Milho e Sorgo, NBA; Universidade Federal de São João del-Rei, Bioengineering</p> <p>Hughes, David; Rothamsted Research, Department of Computational and Analytical Sciences</p> <p>Coelho, Antonio; Empresa Brasileira de Pesquisa Agropecuaria Milho e Sorgo, Soil Fertility</p> <p>Gomes de Paula Lana, Ubiraci; Empresa Brasileira de Pesquisa Agropecuaria Milho e Sorgo, NBA; Centro Universitário de Sete Lagoas, Biology</p> <p>Aparecida Gomes, Eliane; Empresa Brasileira de Pesquisa Agropecuaria Milho e Sorgo, NBA</p> <p>Morais de Sousa, Sylvia; Empresa Brasileira de Pesquisa Agropecuaria Milho e Sorgo, NBA; Universidade Federal de São João del-Rei, Bioengineering; Centro Universitário de Sete Lagoas, Biology</p>
Keywords:	Cerrado, microbiome, maize, metagenomics, rhizosphere, sorghum

SCHOLARONE™  
Manuscripts



# **Crop Type Exerts Greater Influence Upon Rhizosphere Phosphohydrolase Gene Abundance and Phylogenetic Diversity than Phosphorus Fertilization.**

**Andrew L. Neal<sup>1\*</sup>, Timothy McLaren<sup>2</sup>, Mariana Lourenço Campolino<sup>3,4</sup>, David Hughes<sup>5</sup>, Antônio Marcos Coelho<sup>4</sup>, Ubiraci Gomes de Paula Lana<sup>4</sup>, Eliane Aparecida Gomes<sup>4</sup>, Sylvia Moraes de Sousa<sup>3,4\*</sup>**

<sup>1</sup>Department of Sustainable Agricultural Science, Rothamsted Research, North Wyke, EX20 2SB, Devon, United Kingdom.

<sup>2</sup>Department of Environmental Systems Science, Swiss Federal Institute of Technology (ETH), Zürich, Eschikon 33, 8315 Lindau, Switzerland

<sup>3</sup>Universidade Federal de São João del-Rei, R. Padre João Pimentel, 80 - Dom Bosco, São João del-Rei, Minas Gerais, Brazil.

<sup>4</sup>Empresa Brasileira de Pesquisa Agropecuária, Embrapa Milho e Sorgo, Rod. MG 424 KM 65, Sete Lagoas, Minas Gerais, Brazil.

<sup>5</sup>Department of Computational and Analytical Sciences, Rothamsted Research, Harpenden AL5 2JQ, Hertfordshire, United Kingdom.

\*Corresponding authors: ALN - andy.neal@rothamsted.ac.uk; SMS - sylvia.sousa@embrapa.br

## **Abbreviations**

KR – Kantorovich-Rubinstein phylogenetic distance, MSA – multisequence alignment, NMR – nuclear magnetic resonance, NSAP – non-specific acid phosphatase, P0 – unfertilized soil treatment, PD – phylogenetic diversity, PERMANOVA – permutational multivariate analysis of variance, PERMDISP – permutational test of homogeneity of multivariate dispersion, pHMM – profile hidden Markov model, RockP – rock phosphate, PHO – phosphohydrolase, TSP – triple superphosphate,

1  
2  
3  
4  
5  
6  
7  
8  
9  
10  
11  
12  
13  
14  
15  
16  
17  
18  
19  
20  
21  
22  
23  
24  
25  
26  
27  
28  
29  
30  
31  
32  
33  
34  
35  
36  
37  
38  
39  
40  
41  
42  
43  
44  
45  
46  
47  
48  
49  
50  
51  
52  
53  
54  
55  
56  
57  
58  
59  
60

34     **Abstract.**

35     Rock phosphate is considered as an alternative form of phosphorus fertilizer in acidic,  
36     nutrient depleted soils of the Brazilian Cerrado. However, there is no information  
37     regarding the influence of phosphorus fertilizer sources in Cerrado soils upon  
38     microbial genes coding for phosphohydrolase enzymes in crop rhizospheres. Here,  
39     we analyse a field experiment comparing phosphorus fertilization (rock phosphate  
40     and triple superphosphate) of maize and sorghum upon crop performance,  
41     phosphatase activity and rhizosphere microbiomes at three levels of diversity: small  
42     subunit rRNA marker genes of bacteria, archaea and fungi; a suite of alkaline and acid  
43     phosphatase and phytase genes; and ecotypes of individual genes. We showed that  
44     there is no significant difference in crop performance between the fertilizers sources.  
45     Differences in rhizosphere microbiomes were observed at all levels of biodiversity  
46     due to crop type, but not fertilization. Inspection of phosphohydrolase gene ecotypes  
47     responsible for differences between the crops suggests a role for lateral genetic  
48     transfer in establishing ecotype distributions. Our results suggest development of  
49     inocula of microorganisms harbouring the gene ecotypes identified in this study, or  
50     selective breeding of crops with an enhanced capacity to attract beneficial  
51     microorganisms to the rhizosphere may prove useful to optimizing rock phosphate  
52     fertilizer in Cerrado soils.

53     **Key words:** Cerrado, microbiome, maize, metagenomics, rhizosphere, sorghum

54     **Introduction**

55         Due to areas sown and annual production volume, cereals play an important  
56     role in human nutrition, as food and animal feed, and in the world’s agricultural  
57     economy. Maize, wheat and rice are the most widely produced grains, but crops such  
58     as sorghum are especially important in Africa (FAO 2019). The world’s current  
59     population of around 7 billion is estimated to exceed 9 billion by 2050. Challenges to  
60     feed an ever-growing human population – within the context of global climate change  
61     - increase the need for adoption of sustainable and environmentally sound agricultural  
62     practices (FAO 2019; Naumann *et al.* 2018; Ngumbi and Kloepper 2016).

63         Factors that constrain soil fertility and thus, sustainable agriculture, in the  
64     tropics are typically low nutrient capital, water stress, erosion, high phosphorus (P)  
65     sorption and high acidity allied to aluminium toxicity (Camenzind *et al.* 2017;  
66     Garland *et al.* 2018). Soluble P fertilizers applied to soil are often rapidly complexed

via adsorption to iron and aluminium oxides, particularly in clayey tropical soils typical of Cerrado and other Savannah areas worldwide. Such complexation reduces the bioavailability of the added P to plants (Novais and Smyth 1999). P can also be complexed to or within organic compounds which may represent as much as 80% of the total P in no-till soils (Marschner *et al.* 2006). As a result of these processes, organic P pools and decomposition of soil organic matter are critical for sustainable plant productivity in highly weathered tropical soils. The origin, distribution and abundance of genes coding for various families of enzymes associated with the hydrolysis of organic P pools (several families of alkaline and acid phosphatases and phytases) in soils are not particularly well understood, neither is the effect of fertility management upon gene dynamics (George *et al.*, 2018).

Chemical fertilizers, such as manufactured water-soluble phosphate traditionally play a significant role in maintaining pools of bioavailable P in managed agricultural soils. Rising demand for food in developing countries is in turn exerting increased pressure on agricultural land for higher yields and thus increased demand for phosphate fertilizers, leading to an increase in global fertilizer price inflation. Resource-poor farmers are faced with poor-yielding soils which defy costly attempts to improve their nutrient status by fertilization. This puts individual, community and national food security at risk. In addition, intensive use of agricultural inputs can cause environmental impacts such as pollution, soil degradation, micronutrient deficiency, eutrophication of water sources, toxicity to different beneficial organisms and reduction of microbiota biodiversity (Sharma and Singhvi 2017).

In response to these issues, much research has been directed to understanding the role of rock phosphate (RockP) fertilizers in agroecosystems, as it has a relatively low cost and is environmentally less damaging than soluble P (Chien *et al.* 2011). Despite its lower reactivity compared to soluble fertilizers, the P bioavailability of RockP can increase over years of cultivation, due to physicochemical processes and the activity of soil microbiota (Silva *et al.* 2017). Phosphate solubilizing and mineralizing microorganisms have a high potential to be used in the management of P-deficient soils, since they can liberate adsorbed P as a bi-product of organic acid production, and chelate Al and Fe, reducing the precipitation of phosphate minerals (Vega 2007). Many tropical soils naturally support high microbiological activity and

1  
2  
3  
4  
5  
6  
7  
8  
9  
10  
11  
12  
13  
14  
15  
16  
17  
18  
19  
20  
21  
22  
23  
24  
25  
26  
27  
28  
29  
30  
31  
32  
33  
34  
35  
36  
37  
38  
39  
40  
41  
42  
43  
44  
45  
46  
47  
48  
49  
50  
51  
52  
53  
54  
55  
56  
57  
58  
59  
60

biodiversity – much of it under-explored. This diversity could be exploited to counter the challenges associated with food production in highly weathered tropical soils (Cardoso and Kuyper 2006).

Plant roots exude organic compounds including sugars, organic acids, nucleosides, mucilage and amino acids. The resulting concentration gradients can attract microorganisms from the bulk soil to the rhizosphere and to the endosphere (Edwards *et al.* 2015) as well as support higher growth. Plant species exert a strong influence upon rhizosphere microbiomes, but other factors such as soil properties, fertilizers, plant developmental stages, nutritional status of the host plant, and other environmental factors can have confounding effects on rhizosphere microbial communities (Mota *et al.* 2008; Li *et al.* 2014; Bakker *et al.* 2015). Previous work on Brazilian Oxisol Cerrado soils demonstrated that a significant fraction of bacterial and fungal diversity is attributed to the plant host genotype, but in general, the soil P status was the major driver of microbiome structure followed by plant compartment (rhizosphere *versus* rhizoplane-associated) (Gomes *et al.* 2018). This work investigated the i) P chemistry in soils of a long running tropical P fertilizer field trial comparing different sources of P fertilization; ii) phosphatase activity under different crop and fertilizer regimes; and iii) the biodiversity of microbial phosphohydrolase genes involved in organic P cycling.

**Materials and Methods**

*Site description and soil preparation* – The fertilization regimes were established in 2017 in a non-removal soil since 2007 at Embrapa Milho e Sorgo Experimental Station in Sete Lagoas, Minas Gerais, Brazil (19° 28’ S, 44° 15’ W at an altitude of 732 m above sea level). The soil is classified as a Distroferric Red Latosol (Latossolo Vermelho Distroférico) with a clayey texture (Oxisol), under savannah vegetation (Santos *et al.*, 2013) and a pH (H<sub>2</sub>O) of 5.9 in the surface layer (0 – 20 cm). The experiment was under no-till soil management with irrigation when necessary of two continuous crops: sorghum (*Sorghum bicolor* (L.) Moench) and maize (*Zea mays* L.). The field experiment consisted of three fertilizer treatments: 1) plots without addition of fertilizer P [P0]; 2) plots receiving rock phosphate [RockP] (18 % total P<sub>2</sub>O<sub>5</sub> and 4 % soluble in citric acid 2%) at a rate of 100 kg of P<sub>2</sub>O<sub>5</sub> ha<sup>-1</sup> and; 3) fields receiving triple superphosphate [TSP] (45% total P<sub>2</sub>O<sub>5</sub>) at a rate of 100 kg of P<sub>2</sub>O<sub>5</sub> ha<sup>-1</sup> year<sup>-1</sup>.



Soil was sampled in the second season of the experiment (2018/2019), after fertilized plots had received about 44 kg-P ha<sup>-1</sup> yr<sup>-1</sup> or a cumulative 88 kg of P ha<sup>-1</sup>. Prior to establishment of the experiment the field was fallowed under a natural *Brachiaria* pasture between 2007 and 2017. Crops were fertilized at sowing with 40 kg-N ha<sup>-1</sup> and 60 kg-K<sub>2</sub>O ha<sup>-1</sup> and then again as a side dress 30-35 days after planting with 120 kg-N ha<sup>-1</sup> and 60 kg-K<sub>2</sub>O ha<sup>-1</sup>. Micronutrients were not applied because soil analyses indicated that they were at sufficient levels.

The experimental design was a randomized complete block with three replications. For soil samples the area of experimental field was divided in 10 blocks measuring 20 m wide x 18 m long. Before sowing, five soil subsamples were obtained from the experimental field at 20 cm depth from each block and mixed to form a composite soil sample. Measured soil parameters, according to Embrapa (2017): potential acidity (H+Al) = 7.36; calcium (Ca) = 3.03 mg dm<sup>-3</sup>; magnesium (Mg) = 0.47 mg dm<sup>-3</sup>; cation exchange capacity = 10.99 cmol<sub>c</sub> dm<sup>-3</sup>; Mehlich 1 extractable P = 5.16 mg dm<sup>-3</sup>; potassium (K) = 53.8 mg dm<sup>-3</sup>; base saturation = 33.4 % and organic matter (OM) = 36.9 g kg<sup>-1</sup>.

During flowering in 2018/2019, rhizosphere soil was collected from the fine roots of four plants of each crop from each of triplicate treatment plots. After removing weakly adhered soil by manual agitation, 10 g of rhizosphere soil was weighed and frozen in liquid nitrogen. Additional soil from the surface (0 – 20 cm) was sampled, dried and sieved prior to chemical analyses. At cropping, maize cobs and sorghum panicles from the inner crop lines were harvested and threshed by subplot. The resulting grain mass was weighed and corrected for 130 g kg<sup>-1</sup> grain moisture to estimate the total grain yield in Mg ha<sup>-1</sup>.

*Soil organic phosphorus* - Soil organic P was estimated using the method of Cade-Menun and Preston (1996). A total of 2 g of soil was extracted with 40 mL of 0.25 M NaOH + 0.05 M Na<sub>2</sub>-EDTA solution using a horizontal shaker at 160 rpm for 16 h. The extracts were then centrifuged at 5,000 rpm for 20 min., and the supernatant passed through a Whatman no. 42 filter paper. A 20 mL aliquot of the filtrate was frozen at -80 °C, lyophilised and weighed (Doolette *et al.* 2010). This resulted in a mass of lyophilised material ranging from 560 to 574 mg *per* tube across all samples.



162

163 *Solution phosphorus-31 nuclear magnetic resonance (NMR) spectroscopy -*

164 Preparation of lyophilised material for solution  $^{31}\text{P}$  NMR analysis has been described  
165 by Reusser *et al.* (2020). Solution  $^{31}\text{P}$  NMR spectroscopy was carried out on one  
166 replicate of each treatment using a Bruker Avance IIIHD 500 MHz NMR  
167 spectrometer equipped with a 5 mm liquid-state Prodigy™ CryoProbe (Bruker  
168 Corporation; Billerica, MA) at the NMR facility of the Laboratory of Inorganic  
169 Chemistry (Hönggerberg, ETH Zürich). Solution  $^{31}\text{P}$  NMR spectra were acquired at a  
170  $^{31}\text{P}$  frequency of 202.5 MHz and gated broadband proton decoupling with  $90^\circ$  pulses  
171 of 12  $\mu\text{sec}$  duration. Spectral resolution was  $< 0.1$  Hz following sample shimming  
172 across all samples. Two NMR analyses were carried out on all soil samples. The first  
173 was an inversion recovery experiment (Vold *et al.* 1968) to obtain the spin-lattice  
174 relaxation ( $T_1$ ) times of the  $^{31}\text{P}$  NMR signal. The longest  $T_1$  time for each soil sample  
175 was multiplied five-fold and used as the recycle delay of the subsequent  $^{31}\text{P}$  (1D)  
176 NMR analysis. Spin-lattice relaxation times were the longest for orthophosphate  
177 across all soil samples, which ranged from 17 to 29 sec. The average number of scans  
178 across all soil samples was 3,754.

179 *Spectral quantification and identification of peaks* - All NMR spectra were initially  
180 processed with TopSpin® software (Bruker Corporation; Billerica, MA), which  
181 involved spectral phasing and baseline correction. Furthermore, the net peak areas  
182 (integrals) of all  $^{31}\text{P}$  NMR signals were obtained. This generally occurred in the  
183 phosphonate region ( $\delta$  22.02 to 21.98 ppm, 19.81 to 19.76 ppm, 17.02 to 16.31 ppm,  
184 and 14.32 to 14.25 ppm), the combined orthophosphate and phosphomonoester  
185 regions ( $\delta$  6.10 to 2.62 ppm), the phosphodiester region ( $\delta$  0.98 to 0.94 and  $-0.73$  to  
186  $-1.43$  ppm) and the polyphosphate region ( $\delta$   $-4.85$  to  $-4.94$  ppm). The integral of the  
187 NMR signal between  $\delta$  17.02 to 16.31 ppm was that of the added MDP ( $\delta$  16.67 ppm)  
188 including its two  $^{13}\text{C}$  satellite peaks ( $\delta$  16.96 ppm and 16.37 ppm). Due to overlapping  
189 peaks in the combined orthophosphate and phosphomonoester region, spectral  
190 deconvolution and peak fitting was used to partition the NMR signal, following  
191 procedures described by Reusser *et al.* (2020). This involved fitting the region with  
192 between 23 and 50 sharp signals and one broad signal across all samples. Inositol  
193 phosphates were identified by spiking and comparison of spectra to previously spiked

soil extracts using purchased reference materials and compounds from original collections of Dr. Dennis Cosgrove and Dr. Max Tate. The assignment of the broad signal was based on spiking experiments (Reusser *et al.* 2020), transverse relaxation ( $T_2$ ) experiments (McLaren *et al.* 2019), and its isolation in large molecular weight material (McLaren *et al.* 2015).

Quantitative solution  $^{31}\text{P}$  NMR spectra were obtained based on recycle delays allowing for complete relaxation of  $^{31}\text{P}$  nuclei between pulses, and the addition of a known quantity of P as MDP that has a chemical shift separate to that of all other NMR signals in these soil samples. The net peak area of MDP is directly proportional to all other NMR signals. Therefore, quantitative measures of P species on a soil-weight basis were determined using solution  $^{31}\text{P}$  NMR spectroscopy. The proportion of total P in NaOH-EDTA extracts as determined by NMR spectroscopy to that determined by ICP-OES, termed 'NMR observability' (Doolette *et al.* 2011), was on average 82% across all samples in the study.

*DNA extraction, sequencing and quality control* - Soil community DNA was extracted from 10 g of thawed soil of each treatment in triplicate using MoBio PowerSoil® DNA isolation kits (Mo Bio Laboratories, Inc. Carlsbad, CA). DNA quantification and quality was assessed using a Qubit 2.0 fluorimeter (Thermo Fisher Scientific, Waltham, USA) and 2100 Bioanalyzer DNA chips (Agilent Technologies, Santa Clara, USA). A total of 10  $\mu\text{g}$  of high-quality DNA was provided for sequencing for each of the eighteen samples.

Shotgun metagenomic sequencing of DNA was performed using 150 base paired-end chemistry on a BGISEq-500 sequencing platform by BGI (Shenzhen, China). The generated raw sequences were limited to a minimum quality score of 25 and a minimum read length of 70 bases using TRIMMOMATIC (Bolger *et al.* 2014). After filtering to remove substandard sequences, the average number of metagenome reads for each soil was  $4.60 \times 10^8$  under maize - RockP,  $4.57 \times 10^8$  under maize - TSP,  $4.58 \times 10^8$  under maize - P0,  $4.34 \times 10^8$  under sorghum - RockP,  $4.33 \times 10^8$  under sorghum - TSP, and  $4.55 \times 10^8$  under sorghum - P0 (range across all datasets  $3.83 \times 10^8$  –  $4.62 \times 10^8$  reads).

225 *Estimation of gene relative abundance and phylogeny* - Each of the eighteen  
226 metagenomes generated in this study were analysed to assess the phylogenetic  
227 diversity of bacterial, archaeal and fungal small subunit ribosomal RNA genes and  
228 each of nine phosphohydrolase (PHO) genes using methods described by Neal *et al.*  
229 (2017a, b). Nucleotide-based profile hidden Markov models (pHMM) were generated  
230 from multi-sequence alignments (MSAs) of reference sequences of each gene using  
231 HMMBUILD, part of the HMMER suite version 3.1 (Eddy 2009). MSAs for all PHO  
232 genes were generated using the *E-INS-i* iterative refinement algorithm in MAFFT  
233 version 7.3 (Kato and Standley 2013). All MSAs were generated using the 1PAM/ $\kappa$   
234 = 2 scoring matrix. For the 16S rRNA gene, pHMMs were generated from alignment  
235 of a set of 7,245 bacterial and 266 archaeal 16S rRNA reference sequences associated  
236 with PAPRICA version 0.5.2 (Bowman and Ducklow 2015), built November 2019.  
237 For the fungal 18S rRNA gene, a pHMM was generated from 2,447 reference  
238 sequences downloaded from the National Center for Biotechnology Information's  
239 Fungal 18S Ribosomal RNA RefSeq Targeted Loci Project, built February 2020. For  
240 phosphohydrolase genes, pHMMs were generated from 832 *phoD* sequences, 420  
241 *phoX* sequences and 193 *phoA* alkaline phosphatase sequences, 107  $\beta$ -propeller  
242 phytase ( $\beta$ PPhy) sequences, 101 cysteine phytase (CPhy) sequences and 226 histidine  
243 acid phytase (HAPhy) sequences described by Neal *et al.* (2017a), and for 457 class  
244 A, 319 class B and 457 class C of non-specific acid phosphatase (NSAP) sequences  
245 described by Neal *et al.* (2017b). Metagenome reads with homology to each pHMM  
246 were identified using HMMSEARCH and a  $1 \times 10^{-5}$  Expect-value (*E*) cut-off. To allow  
247 meaningful comparison between metagenomic datasets, PHO gene relative abundance  
248 was expressed as a proportion of the estimated total number of genomes in each  
249 dataset, assessed by estimating the abundance of the ubiquitous, single-copy genes  
250 *recA*, *gyrB* (Santos and Ochman 2004) and *atpD* (Gaunt *et al.* 2001). Nucleotide  
251 sequence-based pHMMs were developed for each gene as described in Neal *et al.*  
252 (2017a) using 1,370 reference *recA* sequences, 2,382 reference *gyrB* sequences and  
253 1,330 reference *atpD* sequences. Metagenome-derived homologue counts for each  
254 single-copy gene were size-normalized to the length of the shortest gene pHMM, *recA*  
255 accounting for differences in length between the genes. To do this, the pHMM length  
256 of *recA* (1,164 nt) was divided by the pHMM length of the other single-copy genes  
257 (1,392 nt for *atpD*, and 2,618 nt for *gyrB*), and this value was then multiplied by each  
258 single-copy gene count. The length-normalized abundance of each target

phosphohydrolase gene was then calculated for each soil as [target gene count/read length/(mean normalized counts of single-copy genes)] (Howard *et al.* 2009).

PHMMER was used to compare the retrieved metagenome sequences, following six-frame translation using EMBOSS Transeq (Rice *et al.* 2000), to the UniprotKB protein sequence database to confirm that the sequences represented the correct protein family. Only those metagenome sequences for which one of the six frame translations elicited a UniprotKB hit of the appropriate protein family ( $E < 1 \times 10^{-5}$ ) was included in the subsequent analysis. Metagenome reads showing homology to each gene were assigned to branches of maximum-likelihood (ML) phylogenetic trees generated from the respective reference gene sets using RAxML version 8.2.4 (Stamatakis 2014). Phylogenetic placement was implemented using EPA-NG version 0.3.6 (Barbera *et al.* 2019) and visualized using iTOL version 5.5 (Letunic and Bork 2016). For the bacterial and archaeal 16S rRNA and fungal 18S rRNA genes, these placements can be translated into robust relative abundance estimates of organisms using the taxonomic labelling of the tree branches. This is not the case for PHO genes where instead, placement indicates the degree of homology of metagenome reads (ecotypes) to the respective genes found in sequenced organisms, identified by taxonomic labels of the tree branches.

*Phosphatase activity* - The methods used for assaying the activities of phosphatase enzymes are described by Tabatabai (1994). The methods involve extraction and quantitative determination of  $\mu\text{g}$  *p*-nitrophenol released when soil is incubated with *p*-nitrophenyl phosphate or bis-*p*-nitrophenyl phosphate in modified universal buffer adjusted to pH 6.5 and 11 for acid and alkaline phosphatase, respectively. The reactions were stopped by adding  $\text{CaCl}_2$  and NaOH, the solutions were centrifuged at 8,000 rpm for 5 min. and the supernatant used for colorimetric measurements. Enzyme activities were assayed in triplicate rhizosphere soil samples.

*Statistical Analyses* – To test our hypotheses, we generated gene assemblage-related metrics, including relative abundance, phylogenetic diversity (PD) and phylogeny-based distance metrics. The effects of different fertilizer treatments upon crop yield, grain P accumulation, phosphatase activity and estimates of gene normalized abundance and PD were analysed using a nested analysis of variance (ANOVA) model after testing for homogeneity of variances using Levene's test and normality

1  
2  
3  
4  
5  
6  
7  
8  
9  
10  
11  
12  
13  
14  
15  
16  
17  
18  
19  
20  
21  
22  
23  
24  
25  
26  
27  
28  
29  
30  
31  
32  
33  
34  
35  
36  
37  
38  
39  
40  
41  
42  
43  
44  
45  
46  
47  
48  
49  
50  
51  
52  
53  
54  
55  
56  
57  
58  
59  
60

291 using the Shapiro-Wilk test. The model considered crop type (maize or sorghum) as  
292 the main factor with fertilization (RockP, TSP or P0) nested within crop type. Data  
293 for some genes were associated with significantly non-normal distributions, although  
294 the variances were homogenous. In these instances, permutation-based distribution-  
295 free tests of significance of  $F$ -values were adopted to calculate probability (denoted as  
296  $p_{perm}$ ). We calculated omega squared ( $\omega^2$ ) as an estimate of the extent to which  
297 variance in a response variable was accounted for by the treatment (effect size).  
298 Where significant treatment effects were identified, *post-hoc* pair-wise comparisons  
299 were performed using Tukey-Kramer Studentized  $Q$ , following the Copenhaver-  
300 Holland multiple comparison procedure (Holland and Copenhaver 1988) to control  
301 family-wise Type I error. All parametric tests were performed using PAST version  
302 4.01 (Hammer *et al.* 2001). For all tests, an  $\alpha$  of 0.05 was considered significant.

303       Estimates of gene phylogenetic (that is, sequence similarity-sensitive)  
304 diversity (PD) based upon placement of homologous metagenomic reads were  
305 assessed by computing a measure incorporating abundance, using the FPD binary in  
306 GUPPY version 1.1 (part of the PPLACER code, Matsen *et al.* 2010) accounting for  
307 reference ML tree pendant branch length. The measure equates Faith's PD (McCoy  
308 and Matsen, 2013). To assess the depth of sequencing of the soil communities  
309 compared with the total diversity of the PHO genes within them, rarefaction curves of  
310 expected mean phylogenetic diversity (Nipperess and Matsen, 2013) were generated  
311 using the GUPPY RAREFACT binary, interpreting placement weights as counts and  
312 calculating up to a rarefaction size ( $k$ ) of 70,000. Additionally, unconstrained  
313 ordination based upon principal component analysis of the difference in placement  
314 densities on reference tree branches - termed edge-PCA (Matsen and Evans 2013) -  
315 was used for graphical representation of phylogeny-based differences between  
316 treatments in a two-dimensional plane using the EDGEPCA binary in the GAPPA  
317 code version 0.4.0 (Czech and Stamatakis 2019), treating each query as a point mass  
318 concentrated on the highest-weight placement. An advantage of edge-PCA is that  
319 branches associated with placements contributing to eigenvalues on each axis are  
320 identified and for 16S and 18S rRNA gene analysis, organisms contributing to the  
321 observed differences can be identified. This is not the case for PHO genes where only  
322 association with sequenced homologs can be identified.



To assess 16S rRNA, 18S rRNA and PHO gene-based  $\beta$ -diversity between the different crops and fertilizer treatments, Kantorovich-Rubinstein (KR) phylogenetic distance metrics (Evans and Matsen 2012) were calculated from phylogenetic placements of metagenome reads using the GAPPa KRD binary, treating each query as a point mass concentrated on the highest-weight placement. The KR distance metric, which is allied to the weighted-UniFrac measure (Evans and Matsen 2012), compares gene assemblage distributions on a phylogenetic tree in units of nucleotide substitutions *per site*, a biologically meaningful approach to comparing communities. Differences in gene assemblages based upon KR metrics were tested using permutational multivariate analysis of variance (PERMANOVA, Anderson and ter Braak 2003) following testing for homogeneity of multivariate dispersions among *a priori* groups using PERMDISP (Anderson 2006). The same nested model was adopted for PERMANOVA as described above for ANOVA and significance was based upon 99,999 permutations. Multivariate tests were performed using PRIMER PERMANOVA+ version 7.0.13 (PRIMER-e, Auckland, New Zealand).

## Results

*Crop Performance* – Maize and sorghum were grown in 2018/2019, the second year of P fertilization regimes with TSP and RockP. For maize, there was no statistically significant effect of P fertilization ( $F_{2,6} = 2.2$ ,  $p = 0.197$ ,  $\omega^2 = 0.204$ ) on yield: a mean yield of  $9.64 \pm 0.41$  Mg ha<sup>-1</sup> was achieved across all treatments. A significant effect of P fertilization was observed for sorghum yields ( $F_{2,6} = 9.0$ ,  $p = 0.016$ ,  $\omega^2 = 0.639$ ). In this case, TSP fertilization (yield,  $3.97 \pm 0.19$  Mg ha<sup>-1</sup>) resulted in a significantly greater yield than unfertilized soil (P0 yield,  $3.38 \pm 0.04$  Mg ha<sup>-1</sup>,  $Q = 5.9$ ,  $p = 0.014$ ). Fertilization with RockP resulted in a mean yield of  $3.60 \pm 0.12$  Mg ha<sup>-1</sup>, not significantly different from either of the other two treatments.

*Soil phosphorus* - Concentrations of total NaOH-EDTA extractable P ranged from 277 to 547 mg-P kg<sup>-1</sup> soil, of which 60 - 85% was comprised of inorganic P (Table I). Concentrations of extractable inorganic P were generally higher under maize than sorghum, and under TSP compared to P0. Concentrations of organic P ranged from 81 - 109 mg-P kg<sup>-1</sup> soil, which accounted for 15 - 40% of total extractable P. Concentrations of extractable organic P were generally similar among treatments, but slightly lower under RockP compared to P0 and TSP.

1  
2  
3  
4  
5  
6  
7  
8  
9  
10  
11  
12  
13  
14  
15  
16  
17  
18  
19  
20  
21  
22  
23  
24  
25  
26  
27  
28  
29  
30  
31  
32  
33  
34  
35  
36  
37  
38  
39  
40  
41  
42  
43  
44  
45  
46  
47  
48  
49  
50  
51  
52  
53  
54  
55  
56  
57  
58  
59  
60

Solution <sup>31</sup>P NMR spectra on soil extracts were highly resolved and revealed a plethora of organic P species (Fig. 1). The majority of NMR signal (> 95%) was in the orthophosphate and phosphomonoester regions. The identifiable sharp peaks in these regions, shown in Fig. 1, included: 1) orthophosphate (δ 5.38 ppm); 2) *scyllo*-IP6 (δ 3.26 ppm); 3) four peaks due to *myo*-IP6 (δ 5.06, 4.11, 3.73 and 3.62 ppm); 4) *neo*-IP6 in the 4-equatorial/2-axial position (δ 5.95 and 3.78 ppm); 5) three peaks due to *D-chiro*-IP6 in the 2-equatorial/4-axial position (δ 5.70, 4.30 and 3.88 ppm); 6) *scyllo*-IP5 (δ 3.89, 3.33 and 3.15 ppm); 7) *myo*-IP5 of the (1,2,4,5,6) enantiomer (δ 4.52, 4.01, 3.73, 3.42 and 3.31 ppm); 8) *myo*-IP5 of the (1,3,4,5,6) enantiomer (δ 4.21, 3.62 and 3.31 ppm); and 9) *scyllo*-IP4 (δ 4.30 ppm). In addition, there was an underlying “broad” signal centred at δ 4.10 ppm with a linewidth of 300 Hz. A comparison of <sup>31</sup>P NMR spectra is presented in Fig. 2 and demonstrates a complex but consistent P chemistry in the rhizospheres of both crops under the contrasting fertilization regimes.

Quantification of the various P moieties is presented in Table I. Phosphomonoesters comprised on average 97% of the extractable organic P across the analysed soil. The broad signal (on average 52%) and inositol phosphates (on average 34%) were the predominant pools of phosphomonoesters. Concentrations of the broad signal were generally similar among treatments, but lower under RockP compared to P0 and TSP. Concentrations of IP<sub>6</sub> and lower-order inositol phosphates (i.e. IP<sub>5</sub> and IP<sub>4</sub>) comprised on average 24% and 10% of the total pool of phosphomonoesters and were generally unchanged among the treatments.

*Phosphatase activity* – Sorghum rhizosphere soil supported greater phosphatase activity at both pH 6.5 and 11 (188.0 ± 16.1 and 83.7 ± 11.1 Units L<sup>-1</sup>, respectively) than maize rhizosphere soil (150.0 ± 27.3 and 49.0 ± 12.6 Units L<sup>-1</sup>, respectively). However, the overall effect of crop species upon phosphatase activity at either alkaline ( $F_{1,12} = 1.8, p = 0.200$ ) or acid ( $F_{1,12} = 0.52, p = 0.483$ ) pH was not significant. Significant effects were observed for the different fertilizer applications - nested within crop species - at both alkaline ( $F_{4,12} = 4.2, p = 0.024, \omega^2 = 0.328$ ) and acid ( $F_{1,12} = 6.5, p = 0.005, \omega^2 = 0.484$ ) pH. The effect size associated with fertilization was greater under acid conditions. In both cases, phosphatase activity was greatest in P0 soils and least in soils amended with RockP (Fig. 3).



*Small subunit ribosomal RNA-based community analysis* – Bacterial communities in all soils were dominated (collectively representing > 30% of all reads) by the Acidobacteria *Luteitalea pratensis*, *Candidatus Solibacter usitatus*, *Chloracidobacterium thermophilum* and *Ca. Koribacter versatilis*; the Actinobacteria *Conexibacter woesei* and *Baekduia soli*; the Gemmatimonadete *Gemmatirosa kalamazoonesis*; Proteobacteria including the  $\alpha$ -Proteobacteria *Rhodoplanes* sp. Z2-YC6860 and *Sphingomonas ginsengisoli*, the  $\beta$ -Proteobacteria bacterium GR16-43 and the  $\delta$ -Proteobacterium *Haliangium ochraceum*; the Verrucomicrobium *Ca. Xiphinematobacter* sp.; and the Terribacterium group organism *Thermobaculum terrenum*. Dominant Archaea included the Lokiarchaeote *Ca. Prometheoarchaeum syntrophicum* MK-D1, the Crenarchaeotes *Ca. Mancarchaeum acidiphilum* MIA14, *Ca. Korarchaeum cryptofilum* OPF8, *Desulfurococcus amylolyticus* and *Pyrobaculum arsenaticum*, and the Euryarchaeote Methanomicrobia *Methanotherix soehngenii* and *Methanosaeta harundinacea*. Fungal communities were dominated by the Dothidiomycetes *Brunneoclavispora bambusae* and *Recurvomyces mirabilis*; the Saccharomycete *Starmerella ratchasimensis*; the Mucormycete *Gongronella orasabula*; the Entomophthoromycete *Conidiobolus obscurus*; the Sordariomycetes *Cornuvesica acuminata*, *Dactylidisporea singaporensis* and *D. ellipsospora*; the Umbelopsidomycete *Umbelopsis changbaiensis*; and the Kickxellomycete *Coemansia umbellata*.

Fungal community phylogenetic diversity was largely stable across the experiment (Fig. 4). There was a significant effect of crop type ( $F_{1,12} = 16.8$ ,  $p = 0.001$ ) upon bacterial PD. The maize rhizosphere supported greater PD ( $10,046 \pm 174$ ) than the sorghum rhizosphere ( $8,935 \pm 228$ ), but there was no significant effect of fertilization ( $F_{4,12} = 0.86$ ,  $p = 0.514$ ). A similar trend was observed for archaea: maize supported significantly ( $F_{1,12} = 10.7$ ,  $p = 0.007$ ) higher archaeal PD ( $77,932 \pm 1,199$ ) than sorghum ( $70,805 \pm 1,961$ ), with no significant effect of fertilization ( $F_{4,12} = 0.87$ ,  $p = 0.508$ ). The effect size associated with crop type was larger for bacteria than archaea. For fungi, there was no significant effect of either crop type ( $F_{1,12} = 3.9$ ,  $p = 0.071$ ) or fertilization ( $F_{4,12} = 0.51$ ,  $p = 0.732$ ) upon 18S rRNA-based PD.

There were no statistically significant differences in either bacterial (PERMANOVA,  $pseudo-F_{4,12} = 0.62$ ,  $p_{perm} = 0.620$ ) or archaeal ( $pseudo-F_{4,12} = 0.51$ ,

419  $p_{\text{perm}} = 0.985$ ) 16S rRNA-, or 18S rRNA-based ( $pseudo-F_{4,12} = 0.63$ ,  $p_{\text{perm}} = 0.862$ )  
420 community phylogenetic assemblages ( $\beta$ -diversity) due to fertilization, assessed using  
421 KR distance determined from placement of homologous reads on the respective  
422 phylogenetic trees.

423 Bacterial 16S rRNA-based ( $pseudo-F_{1,12} = 1.7$ ,  $p_{\text{perm}} = 0.127$ ) and fungal  
424 18SrRNA-based ( $pseudo-F_{1,12} = 1.6$ ,  $p_{\text{perm}} = 0.178$ ) assemblages were also not  
425 affected by crop type. However, crop type did influence archaeal 16S rRNA-based  
426 ( $pseudo-F_{1,12} = 2.1$ ,  $p_{\text{perm}} = 0.042$ ) assemblages.

427 To investigate the likely source of these assemblage differences identified by  
428 PERMANOVA of KR distance metrics, we used a multivariate ordination procedure -  
429 edge-PCA – which exploits the phylogenetic structure inherent in the data. Edge-  
430 PCA analysis of the archaeal 16S rRNA homologs indicated several species which  
431 were sensitive to crop type (Fig. 5). Differences were associated with edge-PCA axis  
432 2 which accounted for approximately 20% of total variability. This indicated that  
433 Haloarchaea such as *Natronobacterium gregoryi* together with Methanobacteria  
434 *Methanosaeta* and *Methanothrix*, as well as *Desulfurococcus amylolyticus* were more  
435 associated with maize rhizospheres. The Nitrososphaeraceae *Ca. Nitrososphaera* and  
436 *Ca. Nitrosocosmicus*, *Methanococcus maripaludis*, and the Crenarchaeotes  
437 *Pyrobaculum*, *Acidianus* and *Metallosphaera* were all more associated with sorghum  
438 rhizospheres.

439 *Phosphohydrolase gene abundance and phylogenetic diversity* – Comparison of  
440 phylogenetic rarefaction curves (Supplementary Fig. 1) indicated that all PHO genes  
441 were under-sampled with respect to the total biodiversity in the soils. However,  
442 differences in sampling effort between the different treatments were limited and so  
443 direct comparisons were performed without resorting to rarefaction of the sequence  
444 data, which increases in both Type I and II statistical errors (McMurdie and Holmes  
445 2014). These rarefaction curves also demonstrate the relative phylogenetic diversity  
446 and abundance between the alkaline phosphatases *phoD* and *phoX*, class A and C  
447 nonspecific acid phosphatases and the  $\beta$ -propeller phytase genes in the soils. Genes of  
448 *phoD* were both the most numerous and phylogenetically diverse of the genes, but  
449 *phoX* and the two NSAPs were all similarly numerous and diverse. We assessed  
450 phosphohydrolase gene abundance by normalizing counts with respect to the length-

adjusted counts of three single-copy marker genes; *atpD*, *recA* and *gyrB*. Using this approach, alkaline phosphatase *phoD* and *phoX*, NSAP class A and the  $\beta$ PPHy gene normalized abundances were shown to be different between plant species, all having significantly greater normalized abundance in sorghum rhizospheres than those of maize (Fig. 6), contrary to the limited effects of crop type upon overall community assemblages. Fertilization had no significant influence upon the normalized abundance of any PHO gene. PD of *phoD*, class C NSAPs and  $\beta$ PPHy genes was also sensitive to crop type with sorghum associated with higher PD (Fig. 6). There was no significant effect of fertilization upon PHO PD. The phylogenetic placement of PHO genes showing sensitivity to crop type are shown respectively in Figs. 7 and 8 for the alkaline phosphatases *phoD* and *phoX*, Figs. 9 and 10 for class A and C NSAPs, and Fig. 11 for the  $\beta$ -propeller phytase gene.

KR distance-based assessment of the sensitivity of ecotype assemblages of each PHO gene to crop type and soil fertilization indicated that significant differences in assemblage phylogeny were apparent for all genes except the three phytase families. This indicates a consistent phytase assemblage in all soils considered in this experiment. For the alkaline and non-specific acid phosphatase genes, PERMANOVA identified significant differences in assemblage in response to crop type (smallest  $pseudo-F_{1,12} = 2.0$ ,  $p_{perm} = 0.016$ , *phoX*), but not fertilization. Heterogeneity of multivariate dispersion was only detected for the alkaline phosphatase *phoA* (PERMDISP,  $pseudo-F_{1,2} = 8.9$ ,  $p_{perm} = 0.009$ ) where ecotype assemblages showed reduced heterogeneity in sorghum rhizospheres compared to maize.

For the alkaline phosphatases *phoD* and *phoX* and the two NSAPs for which differences in assemblages due to crop type were observed, we investigated the ecotypes responsible for these differences. For *phoD*, the first two edge-PCA axes accounted for 76% of total phylogenetic variation, separating crops largely on the first axis (Fig. 7). The analysis identified ecotypes with homology to *phoD* genes of a clade of closely related  $\alpha$ -proteobacteria *Sphingopyxis* sp., *Asticcacaulis* sp. and  $\beta$ -proteobacteria *Ralstonia* sp. and *Cupriavidus* sp., and a second closely related clade comprised of the  $\beta$ -proteobacteria *Rhodoferrax ferrireducens* and *Polaromonas* sp. CF318 and a separate clade comprised of the Gemmatimonadetes *Gemmatirosa kalamazoonesis* and *Gemmatimonas* spp. as being more associated with sorghum; and

1  
2  
3  
4  
5  
6  
7  
8  
9  
10  
11  
12  
13  
14  
15  
16  
17  
18  
19  
20  
21  
22  
23  
24  
25  
26  
27  
28  
29  
30  
31  
32  
33  
34  
35  
36  
37  
38  
39  
40  
41  
42  
43  
44  
45  
46  
47  
48  
49  
50  
51  
52  
53  
54  
55  
56  
57  
58  
59  
60

ecotypes with homology to *phoD* genes of a clade of the Actinobacteria *Nocardioides*, *Arthrobacter* and *Streptomyces*, and the  $\gamma$ -proteobacterium *Salinisphaera shabensis* as being more associated with maize. Ecotypes of the alkaline phosphatase *phoX* (Fig. 8) identified as contributing to differences between crop type were again largely associated with edge-PCA axis 1 (accounting for 53% of total variability), but there was a less clear distinction than for *phoD*: in this case ecotypes with homology to *phoX* gene sequences of the  $\alpha$ -proteobacterium *Agrobacterium* sp., the  $\beta$ -proteobacteria *Variovorax paradoxus* B4 and unclassified Methylophilaceae bacterium 11, as well as the  $\gamma$ -proteobacterium *Pseudomonas syringae* were more associated with sorghum, while ecotypes showing homology to a closely related clade comprised of the  $\beta$ -proteobacterium *Ramlibacter tatouinensis* and the  $\alpha$ -proteobacteria *Novosphingobium* sp. and *Asticcacaulis* sp. and the more distantly related *Pseudomonas stutzeri* were all associated more with maize.

Class A NSAP ecotypes showed the greatest separation between crop type on edge-PCA axis 1 (Fig. 9) of all the four PHO genes studied in detail. Combined, the first two axes accounted for 74% of NSAPa phylogenetic variation. Ecotypes sensitive to crop type were dominated by proteobacteria, including those with homology to a large clade of the  $\alpha$ -proteobacterium *Bosea* spp. and the  $\beta$ -proteobacterium *Achromobacter* spp. associated more with maize and a more phylogenetically diverse group of ecotypes including the  $\alpha$ -proteobacterium *Caulobacter* spp., and the  $\beta$ -proteobacteria *Burkholderia* sp. H160 and *B. fungorum*, *Collimonas* sp. and *Herbaspirillum rubrisubalbicans*, all more associated with sorghum. Ecotypes of class C NSAP associating with sorghum also showed homology to genes of the  $\alpha$ -proteobacterium *Thioclava* spp. and the  $\gamma$ -proteobacteria *Xanthomonas* spp. and *Stenotrophomonas* spp. (Fig. 10). In contrast, ecotypes associating with maize showed homology to genes associated Bacteroidetes, including a clade comprised of *Pedobacter* sp. BMA and *Capnocytophaga* sp. and *Flavobacterium* sp. Leaf 82. The first edge-PCA axis accounted for 52% of the total NSAPc phylogenetic variation. Edge-PCA did not identify any clear separation of crop type despite a significant difference in ecotype assemblage.

## 513 Discussion

514 The use of rock phosphates for crop production in acidic, highly weathered  
515 tropical soils such as those found in large regions of South America, Africa and  
516 Australia can be a cost-effective alternative to highly processed phosphate fertilizers  
517 (TSP). This is because RockP is less reactive than TSP and dissolves slowly once  
518 applied to acidic soils, minimizing the rapid complexation of P by iron and aluminium  
519 oxides. Consequently, the use of RockP in place of TSP may shift P utilization of  
520 crops within agricultural systems towards P made bioavailable by the activities of  
521 phosphohydrolase enzymes acting on organic P. However, there is also little  
522 information regarding the effect of P fertilization upon microbial communities  
523 associating with important crops in these soils, or the diversity of genes coding for  
524 phosphohydrolase enzymes in crop rhizospheres. To address these issues, we studied  
525 the performance and response of two economically important crops, maize and  
526 sorghum, to phosphorus fertilization, generating information regarding the speciation  
527 of extractable P and activity of phosphatase enzymes in rhizosphere soils.

528 Crop yields were similar when fertilized with RockP or TSP, which is  
529 consistent with previous observations in Cerrado soils (Silva *et al.* 2017). This  
530 demonstrates that RockP can be an effective source of fertilizer P for crops in Cerrado  
531 soils. Phosphatase activity was the only biological parameter that we observed to be  
532 influenced by P fertilization and significantly higher in the absence of fertilization  
533 (P0) than in fertilized soil at both acid and alkaline pH, but activities were similar  
534 under RockP and TSP fertilization (Fig. 3). There was no association between  
535 phosphatase activity and the abundance or phylogenetic diversity of genes predicted  
536 to code for these enzymes. Despite RockP and TSP having similar effectiveness in  
537 supporting crop yields, the accumulation of fertiliser P into pools of organic soil P  
538 differed between the two fertilised treatments. Slightly lower concentrations of soil  
539 organic P under the RockP treatment compared to the P0 and TSP treatments may be  
540 due to the 'liming' effect of RockP on soil pH (Loganathan *et al.* 2005). The  
541 relatively more alkaline soil pH due to the addition of RockP may have improved  
542 microbial activity and the mobilisation of soil organic P. Complex forms of organic P  
543 (as a broad NMR signal) were the predominant pool of soil organic P that decreased  
544 under the RockP treatment compared to P0 and TSP. This pool of organic P is



1  
2  
3  
4  
5  
6  
7  
8  
9  
10  
11  
12  
13  
14  
15  
16  
17  
18  
19  
20  
21  
22  
23  
24  
25  
26  
27  
28  
29  
30  
31  
32  
33  
34  
35  
36  
37  
38  
39  
40  
41  
42  
43  
44  
45  
46  
47  
48  
49  
50  
51  
52  
53  
54  
55  
56  
57  
58  
59  
60

545 associated with P in large supra-macromolecular structures as part of the soil organic  
546 matter. Consequently, the mobilisation of P within soil organic matter may be an  
547 important source of P in these soils when P is limiting crop growth.

548 A diverse range of inositol phosphates, including lower-order inositol  
549 phosphates (*i.e.* IP<sub>5</sub> and IP<sub>4</sub>) were detected in these soils, comprising about one third  
550 of the total pool of organic P. Since concentrations of inositol phosphates remained  
551 unchanged among treatments, their bioavailability appears to be low in these soils,  
552 and may also reflect the low relative abundance of genes coding for phytate in these  
553 soils (Fig.6, supplementary Fig. 1).

554 Pools of NaOH-EDTA extractable inorganic P in soil are considered to be that  
555 of aluminium and iron phosphates, and pools of P sorbed to mineral surfaces (Novais  
556 and Smyth 1999). Concentrations of extractable inorganic P increased in the RockP  
557 and TSP treatments compared to P0 for maize, which suggest much of the added  
558 fertiliser P was sorbed by the soil and unavailable for plant uptake. This would be  
559 consistent with the crop yield data, which remained unchanged for maize. However,  
560 concentrations of inorganic P increased to a lesser extent for TSP, and remained  
561 largely unchanged for Rock P, when compared to the P0 sorghum. It is likely that the  
562 exudation of low molecular weight organic acids by sorghum resulted in a greater  
563 mobilization of sorbed P, which could then be taken up by the crop (Jones 1998;  
564 Johnson and Loeppert 2005).

565 The principal mechanisms employed by plants in response to low-P  
566 bioavailability in soil are modulation of high-affinity P transporters and exudation or  
567 secretion of organic acids and phosphatases to liberate orthophosphate from inorganic  
568 and organic complexes respectively. Root morphology modifications leading to an  
569 increase in fine roots capable of efficient mining of soil for P also enhances uptake  
570 and grain yield in tropical soils with low P availability (Hufnagel *et al.* 2014). Root  
571 morphological changes, together with organic acid exudation and phosphatase  
572 secretion can influence the abundance and species richness of microbial communities  
573 thought to aid plants in acquiring P from soil (López-Arredondo *et al.* 2014).

574 A diverse group of organisms were found associated with the rhizosphere of  
575 the crops in this study. Actinobacteria are well adapted to dry environments such as

well-drained oxisols since they have evolved strategies, including sporulation and encystment, to survive extreme water stress (Soina, *et al.* 2004; Mohammadipanah and Wink 2016), as well as low pH (Khan and Williams 1975). It is therefore not surprising to find that several dominant bacteria in the crop rhizospheres in these Cerrado soils were Actinobacteria. Similarly, it is also not unusual to identify several dominant Acidobacteria, which are particularly well adapted to oligotrophic, acidic soils (Kielak *et al.* 2016). Actinobacteria often harbour suites of enzymes necessary to degrade plant biomass and they are probably important for terrestrial carbon cycling (Lewin *et al.* 2016). The Gemmatimonadetes organism *Gemmatirosa kalamazoonesis* is a representative of a group of extremely abundant soil bacteria which are well-adapted to arid conditions, constituting as much as 2% of global soil communities (DeBruyn *et al.* 2011). The bacterial communities in these soils therefore appears very typical of soil communities from around the world. Of the dominant archaeal species, two are dependent upon close association with other organisms. *Ca.* *Prometheoarchaeum syntrophicum* MK-D1 is a slow growing anaerobic organism that degrades amino acids syntrophically in association with other archaea - *Halodesulfovibrio* and *Methanogenium* in the original co-cultures - through interspecies hydrogen (and/or formate) transfer (Imachi *et al.* 2020). A second mesothermophilic organism, *Ca.* *Mancarchaeum acidiphilum* MIA14, also degrades proteins and amino acids as part of an obligate partner-dependent lifestyle (Golyshina *et al.* 2017) and its genome lacks any genes of the central carbohydrate metabolism pathways. Free-living *Ca.* *Korarchaeum cryptofilum* OPF8 grows heterotrophically, but also using a variety of peptide and amino acid degradation pathways (Elkins *et al.* 2008). Fungal communities were dominated by poorly studied organisms, none of which have been documented to have a mycorrhizal lifestyle. These included the bamboo-associating *Brunneoclavispora bambusae* and *Recurvomyces mirabilis*, a rock-inhabiting fungus of semi-arid environments (Selbmann *et al.* 2008). Several of the most abundant fungi exhibit biotrophy, including the obligate aphid pathogen *Conidiobolus obscurus* (Wang *et al.* 2018) and *Cornuvesica acuminata*, *Dactylidisporea singaporensis* and *D. ellipsospora* all of which are mycoparasites and typically isolated from soils (Marin-Felix *et al.* 2018). Identification of the Mucormycete *Gongronella orasabula* is potentially significant for P-acquisition by crops in these soils as a congener, *Gongronella* sp. w5, is a putative biotrophic fungus



609 that may promote plant growth by secreting organic acids, facilitating plant phosphate  
610 acquisition (Dong *et al.* 2018).

611 Despite the limited difference in rhizosphere communities associated with the  
612 crops based on small subunit ribosomal RNA (SSU rRNA) gene KR distance metrics,  
613 bacterial, archaeal and fungal community median PD was consistently greater in  
614 maize rhizospheres than sorghum (Fig. 4). In stark contrast, all phosphohydrolase  
615 genes studied in detail were both more abundant and exhibited greater PD in sorghum  
616 rhizospheres (Fig 6). This is a salient finding: it demonstrates that the abundance and  
617 PD of genes coding for these important enzymes respond independently of  
618 community marker genes. This phenomenon has been observed before in cultivated  
619 soils growing winter wheat (Neal and Glendining 2019). Comparing  
620 phosphohydrolase genes in UK agricultural soils maintained at a minimum soil pH of  
621 7.0–7.5 with calcium carbonate addition to promote plant health with the more acidic  
622 Cerrado soils suggests that the general phylogenetic diversity of genes differs between  
623 the soils: specifically, the estimated mean PD of alkaline phosphatase *phoX* genes is  
624 greater than either of the NSAP classes in UK agricultural soil (Supplementary Fig. 2,  
625 Neal and Glendining 2019), but the three genes have similar estimated mean PD in  
626 Cerrado soils (Supplementary Fig. 1). Observations of variable gene diversity in soils  
627 from a wide variety of geographical locations with a wide variety of P-chemistry and  
628 availability have been observed before (Ragot *et al.* 2017). This variability may  
629 simply reflect the prevailing pH in UK and Cerrado soils. However, Neal and  
630 Glendining (2019) noted that alkaline phosphatases PhoD and PhoX and the  $\beta$ PPHy  
631 enzymes all require calcium as a co-factor and low calcium bioavailability may be  
632 associated with an increase in PHO genes coding for enzymes that do not require  
633 calcium cofactor, such as NSAPs: Cerrado soils are characteristically low in  
634 bioavailable calcium (Lopes and Guilherme 2016) and the increased NSAP diversity  
635 observed in these soils would be consistent with calcium exerting a degree of  
636 influence upon wider phosphohydrolase gene diversity.

637 It is evident that neither the levels (P0 vs. [RockP, STP]) nor the quality  
638 (RockP vs. STP) of P fertilization exerted any significant influence upon the  
639 abundance or PD of phosphohydrolase genes. It is well recognized that plants release  
640 complex mixtures of relatively structurally simple compounds from their roots into

the surrounding soil which may attract quite distinct communities of microorganisms to the rhizosphere (Neal *et al.* 2012; Schlemper *et al.* 2017; Hu *et al.* 2018; Miller *et al.* 2019). These microorganisms can increase orthophosphate supply to plants by hydrolysis of organic P through the action of phosphatases, especially phytases (Richardson and Simpson 2011) or by RockP solubilization through organic acid production (Mendes *et al.* 2014). Both maize and sorghum are also known to secrete phosphatase enzymes into the rhizosphere (Furlani *et al.* 1984; Machado and Furlani 2004). We only included rhizosphere soil and communities here and so cannot comment on how they differ from the background soil communities. However, if rhizosphere selection occurred it is evident that maize and sorghum attract and support phylogenetically similar communities. It is then hard to reconcile the observed increases in abundance and PD of phosphohydrolase genes with the limited changes in community structure: we conjecture that it is in fact genes themselves that become more abundant because they confer competitive advantage to individual cells rather than species within the confines of the sorghum rhizosphere, where the genes are collectively both more abundant and phylogenetically diverse. This would require lateral transfer of genes between community members (Maheshwari *et al.* 2017). Inspection of the PHO gene ecotypes identified as responsive to the different crop types by edge-PCA (Figs. 7 - 10) corroborates this notion: many of the responsive ecotypes form clades of closely related phosphohydrolase gene sequences which are found in phylogenetically distinct organisms – most commonly from different classes of the proteobacteria. For example, the phylogenetically close *phoD* gene sequences found in the  $\alpha$ -proteobacteria *Sphingopyxis* and *Asticcacaulis* and the  $\beta$ -proteobacteria *Ralstonia* and *Cupriavidus* which are identified as associating more with the sorghum rhizosphere (Fig. 7), or the phylogenetically close NSAPa gene sequences found in the  $\alpha$ -proteobacterium *Bosea* and  $\beta$ -proteobacterium *Achromobacter* which associate more with maize (Fig. 9).

Despite reduced solubility, RockP can be an effective P-fertilizer in tropical environments, especially regarding the surficial reactions between the mineral and soil solution, which are intensified at the temperatures and humidity in tropical soils (Trabelsi *et al.* 2017). However, depending on the properties of RockP, soil, climatic conditions, crops and management practices, up to four years of annual application are required for RockP to be as effective as soluble phosphates (Ghani *et al.* 1994).

1  
2  
3  
4  
5  
6  
7  
8  
9  
10  
11  
12  
13  
14  
15  
16  
17  
18  
19  
20  
21  
22  
23  
24  
25  
26  
27  
28  
29  
30  
31  
32  
33  
34  
35  
36  
37  
38  
39  
40  
41  
42  
43  
44  
45  
46  
47  
48  
49  
50  
51  
52  
53  
54  
55  
56  
57  
58  
59  
60

674 Our study was performed in the second year of continuous RockP application,  
675 suggesting it is feasible in terms of crop yield to use RockP as an alternative P source  
676 instead of soluble P fertilizers over the long-term. However, in soils with high P-  
677 adsorption and low ion exchange capacities, such as the Brazilian Oxisols studied  
678 here, short-term direct use of RockP as fertilizers for annual crops may be less  
679 economically viable. One option to overcome this would be to use partially acidulated  
680 rock phosphates, and either inocula of selected microorganisms harbouring gene  
681 ecotypes identified in this study, or selective breeding of crops with an enhanced  
682 capacity to attract beneficial microorganisms to the rhizosphere.

683 **Acknowledgements**

684 This work was supported by Empresa Brasileira de Pesquisa Agropecuária - Embrapa  
685 (Grant No 12.14.10.003.00.00) and a Biotechnology and Biological Science Research  
686 Council (BBSRC)/Newton-funded UK-Brazil Alliance for Sustainable Agriculture  
687 award. ALN and DH are supported by the BBSRC-funded *Soil to Nutrition* strategic  
688 programme (BBS/E/C/000I0310) and the Natural Environment Research Council and  
689 BBSRC as part of the *Achieving Sustainable Agricultural Systems* research  
690 programme (NE/N018125/1 LTS-M). MLC is a recipient of a research fellowship  
691 from Coordenação de Aperfeiçoamento de Pessoal de Nível Superior – Capes. The  
692 authors would like to thank Dr. Ajit Singh (Department of Computational and  
693 Analytical Sciences, Rothamsted Research) for maintaining the Metagenomics  
694 Galaxy workflows used here, Dr. René Verel of the Laboratory of Inorganic  
695 Chemistry (Hönnigerberg, ETH Zürich) and Dr. Laurie Paule Schönholzer of the  
696 Group of Plant Nutrition (Eschikon, ETH Zürich) for technical assistance. Authentic  
697 samples of *myo*-, *scyllo*-, *neo*-, and *chiro*-inositol hexakisphosphate were acquired  
698 from the original collections of Dr. Dennis Cosgrove and Dr. Max Tate.

699 **References**

700 Anderson M, ter Braak C. Permutation tests for multi-factorial analysis of variance. *J*  
701 *Stat Comput Sim* 2003; 73: 85-13, DOI: 10.1080/00949650215733.

702 Anderson, MJ. Distance-based tests for homogeneity of multivariate dispersions.  
703 *Biometrics* 2006; 62: 245-53, DOI: 10.1111/j.1541-0420.2005.00440.x.

- 704 Bakker MG, Chaparro JM, Manter DK et al. Impacts of bulk soil microbial  
705 community structure on rhizosphere microbiomes of *Zea mays*. *Plant Soil* 2015;  
706 392:115-26, DOI: 10.1007/s11104-015-2446-0.
- 707 Barbera P, Kozlov AM, Czech L, et al. EPA-ng: massively parallel evolutionary  
708 placement of genetic sequences. *Systematic Biology* 2019; 68:365–69, DOI: 10.1093 /  
709 sysbio / syy054.
- 710 Bolger AM, Lohse M, Usadel B. Trimmomatic: a flexible trimmer for Illumina  
711 sequence data. *Bioinformatics* 2014; 30:2114–20,  
712 DOI:10.1093/bioinformatics/btu170.
- 713 Bowman JS, Ducklow HW. Microbial communities can be described by metabolic  
714 structure: a general framework and application to a seasonally variable, depth-  
715 stratified microbial community from the coastal West Antarctic Peninsula. *PLoS One*  
716 2015; 10, DOI: 10.1371/journal.pone.0135868.
- 717 Cade-Menun B, Preston C. A comparison of soil extraction procedures for <sup>31</sup>P NMR  
718 spectroscopy. *Soil Sci* 1996; 161: 770-85, DOI:10.1097/00010694-199611000-00006.
- 719 Camenzind T, Hättenschwiler S, Treseder K et al. Nutrient limitation of soil  
720 microbial processes in tropical forests. *Ecol Monog* 2017; DOI: 10.1002/ecm.1279.
- 721 Cardoso IM, Kuyper TW. Mycorrhizas and tropical soil fertility. *Agric Ecosyst*  
722 *Environ* 2006; 116: 72-84, DOI:10.1016/j.agee.2006.03.011.
- 723 Chien S.H., Prochnow L.I., Tu S., Snyder C.S. Agronomic and environmental aspects  
724 of phosphate fertilizers varying in source and solubility: an update review. *Nutr. Cycl.*  
725 *Agroecosyst.* 2011; 89:229–255.
- 726 Czech L, Stamatakis A. Scalable methods for analysing and visualizing phylogenetic  
727 placement of metagenomic samples. *PLoS One* 2019; 14, DOI:  
728 0.1371/journal.pone.0217050.
- 729 DeBruyn JM, Nixon LT, Fawaz MN et al. Global biogeography and quantitative  
730 seasonal dynamics of Gemmatomonadetes in soil. *Appl Environ Microbiol* 2011;  
731 77:6295-00, DOI: 10.1128/AEM.05005-11.

- 732 Dong W, Bhide Y, Marsman S et al. Monophosphoryl lipid a-adjuvanted virosomes  
733 with Ni-chelating lipids for attachment of conserved viral proteins as cross-protective  
734 influenza vaccine. *Biotechnol J* 2018; 1700645:1–9, DOI:  
735 10.1016/j.jbiotec.2018.08.022.
- 736 Doolette AL, Smernik RJ, Dougherty WJ. Overestimation of the importance of  
737 phytate in NaOH–EDTA soil extracts as assessed by  $^{31}\text{P}$  NMR analyses. *Org.*  
738 *Geochem* 2011; 42:955-64, DOI: 10.1016/j.orggeochem.2011.04.004.
- 739 Doolette AL, Smernik RJ, Dougherty WJ. Rapid decomposition of phytate applied to  
740 a calcareous soil demonstrated by a solution  $^{31}\text{P}$  NMR study. *Eur. J. Soil Sci* 2010;  
741 61:563-75, DOI: 10.1111/j.1365-2389.2010.01259.x.
- 742 Eddy S. A new generation of homology search tools based on probabilistic inference.  
743 *Genome informatics* 2009; 23:05-11, DOI:10.1142/9781848165632\_0019.
- 744 Edwards J, Johnson C, Santos-Medellín C et al. Structure, variation, and assembly of  
745 the root-associated microbiomes of rice. *Proc. Natl Acad. Sci* 2015; 112:911–20,  
746 DOI: 10.1073/pnas.1414592112.
- 747 Elkins JG, Podar M, Graham DE et al. A korarchaeal genome reveals insights into the  
748 evolution of the Archaea. *PNAS* 2008; 105: 8102-07, DOI:  
749 10.1073/pnas.0801980105.
- 750 Embrapa. Centro Nacional de Pesquisa de Solos. Manual de métodos de análise de  
751 solo. 3. Ed. Rio de Janeiro, 2017. (Embrapa – CNOS. Documento).
- 752 Evans SN, Matsen FA. The phylogenetic Kantorovich-Rubinstein metric for  
753 environmental sequence samples. *J R Stat Soc Series B Stat Methodol* 2012;74:569–  
754 92, DOI:10.1111/j.1467-9868.2011.01018.x.
- 755 FAO - Food and Agriculture Organization on the United Nations. <http://www.fao.org/>  
756 The State of Food and Agriculture 2019. Moving forward on food loss and waste  
757 reduction.

- 758 Furlani A, Clark R, Maranville J et al. Root phosphatase activity of sorghum  
759 genotypes grown with organic and inorganic sources of phosphorus. *J Plant Nutr*  
760 1984; 7:1583-95, DOI:10.1080/01904168409363304.
- 761 Gandhi N.U., Chandra S.B. A comparative analysis of three classes of bacterial non-  
762 specific acid phosphatases and archaeal phosphoesterases: evolutionary perspective.  
763 *Acta Informatica Medica* 2012; 20, 167-173.
- 764 Garland NT, McLamore ES, Cavallaro ND et al. Flexible laser-induced graphene for  
765 nitrogen sensing in soil. *ACS Appl Mater Interfaces* 2018; 10:39124–33, DOI:  
766 10.1021/acsami.8b10991.
- 767 Gaunt MW, Turner SL, Rigottier-Gois L et al. Phylogenies of *atpD* and *recA* support  
768 the small subunit rRNA-based classification of rhizobia. *Int J Syst Evol Microbiol*  
769 2001; 51:2037-48, DOI: 10.1099 / 00207713-51-6-2037.
- 770 George TS, Giles CD, Menezes-Blackburn D. *et al.* Organic phosphorus in the  
771 terrestrial environment: a perspective on the state of the art and future priorities. *Plant*  
772 *Soil* 2018; 427:191–08, DOI:10.1007/s11104-017-3391-x.
- 773 Ghani A, Rajan SSS, Lee A. Enhancement of phosphate rock solubility through  
774 biological processes. *Soil Biol Biochem* 1994; 26:127-36.
- 775 Golyshina OV, Toshchakov S, Makarova KS. 'ARMAN' archaea depend on  
776 association with euryarchaeal host in culture and *in situ*. *Nature Communications*  
777 2017; 8:60, DOI:10.1038/s41467-017-00104-7.
- 778 Gomes EA, Lana UGP, Quensen JF et al. Root-associated microbiome of maize  
779 genotypes with contrasting phosphorus use efficiency. *Phytobiomes J* 2018; 2:129-37,  
780 DOI: 10.1094/PBIOMES-03-18-0012-R.
- 781 Hammer Ø, Harper D, Ryan P. PAST: Paleontological Statistics Software Package for  
782 Education and Data Analysis. *Palaeontol Electron* 2001; 4:1-9.
- 783 Holland BS, Copenhaver MD. "Improved Bonferroni-type multiple testing  
784 procedures": Correction to Holland and Copenhaver. *Psychological Bulletin* 1988;  
785 104:299, DOI: 10.1037/0033-2909.104.2.299.



- Howard E, Shulei F, Erin M et al. Abundant and diverse bacteria involved in DMSP degradation in marine surface waters. *Environ Microbiol* 2008; 10:2397-10, DOI:10.1111/j.1462-2920.2008.01665.x.
- Hu L, Robert CAM, Cadcot S et al. Root exudate metabolites drive plant-soil feedbacks on growth and defense by shaping the rhizosphere microbiota *Nat. Commun* 2018; 9: 2738, DOI: 10.1038/s41467-018-05122-7.
- Hufnagel B, de Sousa, Assis L et al. Duplicate and Conquer: Multiple Homologs of *PHOSPHORUS-STARVATION TOLERANCE1* Enhance Phosphorus Acquisition and Sorghum Performance on Low-Phosphorus Soils. *Plant Physiology* 2014; 166:659-77; DOI: 10.1104/pp.114.243949.
- Imachi H, Nobu MK, Nakahara, N. et al. Isolation of an archaeon at the prokaryote–eukaryote interface. *Nature* 2020; 577:519–25, DOI:10.1038/s41586-019-1916-6.
- Johnson SE, Loeppert RH. Role of organic acids in phosphate mobilization from iron oxide. *Soil Sci Soc Am J* 2005; 70:222-34, DOI: 10.2136/sssaj2005.0012.
- Jones D. Organic acids in the rhizosphere – a critical review. *Plant Soil* 1998; 205:25-44, DOI: 10.1023/A:1004356007312.
- Katoh K, Standley DM. MAFFT Multiple Sequence Alignment Software Version 7: Improvements in performance and usability. *Mol Biol Evol* 2013; 30: 772-80, DOI: 10.1093/molbev/mst010.
- Khan MR, Williams ST. Studies on the ecology of actinomycetes in soil—VIII: Distribution and characteristics of acidophilic actinomycetes. *Soil Biol Biochem* 1975; 7:345-48, DOI: 10.1016/0038-0717(75)90047-4.
- Kielak AM, Barreto CC, Kowalchuk GA et al. The ecology of Acidobacteria: moving beyond genes and genomes. *Front Microbiol* 2016; 7:744, DOI: 10.3389/fmicb.2016.00744.
- Letunic I, Bork P. Interactive Tree of Life (iTOL) v3: An Online Tool for the Display and Annotation of Phylogenetic and Other Trees. *Nuc Acid Res* 2016; 44: 242-45, DOI: 10.1093/nar/gkw290 .



- 814 Lewin GR, Carlos C, Chevrette MG et al. Evolution and ecology of Actinobacteria  
815 and their bioenergy applications. *Annu Rev Microbiol* 2016; 70:235–54,  
816 DOI:10.1146/annurev-micro-102215-095748.
- 817 Li X, Rui J, Xiong J, et al. Functional potential of soil microbial communities in the  
818 maize rhizosphere. *PLoS One* 2014; 9, DOI: 10.1371/journal.pone.0112609.
- 819 Lim B.L., Yeung P., Cheng C., Hill J.E. Distribution and diversity of phytate-  
820 mineralizing bacteria. *ISME J* 2007; 1, 321-30, DOI: [10.1038/ismej.2007.40](https://doi.org/10.1038/ismej.2007.40).
- 821 Loganathan P, Hedley MJ, Bolan NS et al. Field evaluation of the liming value of two  
822 phosphate rocks and their partially acidulated products after 16 years of annual  
823 application to grazed pasture. *Nutr Cycl Agroecosyst* 2005; 72: 287–97, DOI:  
824 [10.1007/s10705-005-4277-5](https://doi.org/10.1007/s10705-005-4277-5).
- 825 Lopes AR, Guimarães GLR. Chapter One - A career perspective on soil management  
826 in the Cerrado Region of Brazil. *Adv Agron* 2016; 137: 1-72,  
827 DOI:10.1016/bs.agron.2015.12.004.
- 828 López-Arredondo D, Leyva-González M, González-Morales S. Phosphate Nutrition:  
829 Improving Low-Phosphate Tolerance in Crops. *Ann Rev Plant Biol* 2014; 65,  
830 DOI:10.1146/annurev-arplant-050213-035949.
- 831 Machado CTT, Furlani AMC. Root phosphatase activity, plant growth and  
832 phosphorus accumulation of maize genotypes. *Sci Agric* 2004; 61:216-23, DOI:  
833 [10.1590/S0103-90162004000200015](https://doi.org/10.1590/S0103-90162004000200015).
- 834 Maheshwari M and Abulreesh, Hussein and Khan, Mohammad and Ahmad et al.  
835 Horizontal Gene Transfer in Soil and the Rhizosphere: Impact on Ecological Fitness  
836 of Bacteria. 2017, DOI: [10.1007/978-981-10-5589-8\\_6](https://doi.org/10.1007/978-981-10-5589-8_6).
- 837 Majumdar A, Ghatak A, Ghosh RK. Identification of the gene for the monomeric  
838 alkaline phosphatase of *Vibrio cholerae* serogroup O1 strain. *Gene* 2005; 344: 251–  
839 58, DOI: [10.1016/j.gene.2004.11.005](https://doi.org/10.1016/j.gene.2004.11.005).

- Marin-Felix Y, Guarro J, Ano-Lira JF et al. *Melanospora* (Sordariomycetes, Ascomycota) and its relatives. *MycoKeys* 2018; 44:81-22, DOI: 10.3897/mycokeys.44.29742.
- Marschner P, Solaiman Z, Rengel Z. Rhizosphere properties of Poaceae genotypes under P-limiting conditions. *Plant Soil* 2006; 283: 11-24, DOI: 10.1007/s11104-005-8295-5.
- Matsen FA, Evans SN. Edge principal components and squash clustering: using the special structure of phylogenetic placement data for sample comparison. *PLoS One* 2013; 8: e56859, DOI: 10.1371/annotation/40cb3123-845a-43e7-b4c0-9fb00b6e2212.
- Matsen FA, Kodner RB, Armbrust EV. pplacer: linear time maximum-likelihood and Bayesian phylogenetic placement of sequences onto a fixed reference tree. *BMC Bioinformatics* 2010;11:538, DOI: 10.1186/1471-2105-11-538.
- McCoy CO, Matsen FA 4th. Abundance-weighted phylogenetic diversity measures distinguish microbial community states and are robust to sampling depth. *PeerJ*. 2013;1:157, DOI: 10.7717/peerj.157.
- McLaren TI, Smernik RJ, McLaughlin MJ, et al. Complex forms of soil organic phosphorus – a major component of soil phosphorus. *Environ. Sci. Technol* 2015; 49:13238–45, DOI: 10.1021 / acs.est.5b02948.
- McLaren TI, Verel R, Frossard E. The structural composition of soil phosphomonoesters as determined by solution <sup>31</sup>P NMR spectroscopy and transverse relaxation (T<sub>2</sub>) experiments. *Geoderma* 2019; 345: 31-37, DOI: 10.1016/j.geoderma.2019.03.015.
- McMurdie PJ, Holmes S. Waste not, want not: why rarefying microbiome data is inadmissible. *PLoS Comput Biol* 2014; 10, DOI:10.1371/journal.pcbi.1003531.
- Mendes GO, de Freitas ALM, Pereira OL. Mechanisms of phosphate solubilization by fungal isolates when exposed to different P sources. *Ann. Microbiol* 2014; 64:239–49. DOI: 10.1007/s13213-013-0656-3.

- 867 Miller SB, Heuberger AL, Broeckling CD et al. Non-Targeted metabolomics reveals  
868 Sorghum rhizosphere-associated exudates are influenced by the belowground  
869 interaction of substrate and Sorghum genotype. *Int J Mol Sci* 2019; 20:431, DOI:  
870 10.3390/ijms20020431.
- 871 Mohammadipanah F and Wink J. Actinobacteria from arid and desert habitats:  
872 diversity and biological activity. *Front. Microbiol* 2010; 6:1541, DOI:  
873 10.3389/fmicb.2015.01541.
- 874 Monds R, Newell P, Schwartzman J et al. Conservation of the Pho regulon in  
875 *Pseudomonas fluorescens* Pf0-1. *Appl. Environ. Microbiol.* 2006; 72. 1910-24,  
876 DOI:10.1128/AEM.72.3.1910-1924.2006.
- 877 Mota D, Faria F, Gomes EA et al. Bacterial and fungal communities in bulk soil and  
878 rhizospheres of aluminum-tolerant and aluminum-sensitive maize *Zea mays* L. lines  
879 cultivated in unlimed and limed Cerrado soil. *J. Microbiol. Biotechnol* 2008; 18:805-  
880 14.
- 881 Naumann G, Alfieri L, Wyser K et al. Global changes in drought conditions under  
882 different levels of 819 warming. *Geophys Res Lett* 2018; 45:3285-96,  
883 DOI:10.1002/2017GL076521.
- 884 Neal AL, Ahmad S, Gordon-Weeks R, Ton J. Benzoxazinoids in root exudates of  
885 maize attract *Pseudomonas putida* to the rhizosphere. *PLoS One* 2012;7:e35498,  
886 DOI:10.1371/journal.pone.0035498.
- 887 Neal AL, Blackwell M, Akkari E. et al. Phylogenetic distribution, biogeography and  
888 the effects of land management upon bacterial non-specific Acid phosphatase Gene  
889 diversity and abundance. *Plant Soil* 2017b; 427:175–89, DOI: 10.1007/s11104-017-  
890 3301-2.
- 891 Neal AL, Glendining MJ. Calcium exerts a strong influence upon phosphohydrolase  
892 gene abundance and phylogenetic diversity in soil. *Soil Biol Biochem* 2019; 139, DOI:  
893 10.1016/j.soilbio.2019.107613.

- 894 Neal AL, Rossmann M, Brearley C et al. Land-use influences phosphatase gene  
895 microdiversity in soils. *Environ Microbiol* 2017a; 19: 2740-53, DOI:10.1111/1462-  
896 2920.13778.
- 897 Ngumbi E, Kloepper J. Bacterial-mediated drought tolerance: current and future  
898 prospects. *Appl. Soil Ecol* 2016; 105: 109–25, DOI: 10.1016/j.apsoil.2016.04.009.
- 899 Nipperess DA, Matsen FA. The mean and variance of phylogenetic diversity under  
900 rarefaction. *Methods Ecol Evol* 2013; 4:566-72, DOI:10.1111/2041-210X.12042.
- 901 Novais RF; Smyth TJ. Fósforo no solo e nas plantas em condições  
902 tropicais. Universidade Federal de Viçosa, Viçosa, MG, Brasil, 1999. 309 p.
- 903 Ragot SA, Kertesz MA, Mészáros E et al. Soil *phoD* and *phoX* alkaline phosphatase  
904 gene diversity responds to multiple environmental factors, *FEMS Microbiol Ecol*  
905 2017; 93:212, DOI: doi.org/10.1093/femsec/fiw212.
- 906 Reusser JE, Verel R, Frossard E et al. Quantitative measures of *myo*-IP<sub>6</sub> in soil using  
907 solution <sup>31</sup>P NMR spectroscopy and spectral deconvolution fitting including a broad  
908 signal. *Environ Sci Process Impacts* 2020, DOI:10.1039/C9EM00485H.
- 909 Rice P, Longden I, Bleasby A. EMBOSS: The European molecular biology open  
910 software suite. *Trends Genet* 2000; 16:276-87, DOI:10.1016/S0168-9525(00)02024-  
911 2.
- 912 Richardson AE, Simpson RJ. Soil microorganisms mediating phosphorus availability  
913 update on microbial phosphorus. *Plant Physiol* 2011; 156:989–96, DOI:  
914 10.1104/pp.111.175448.
- 915 Santos HG, Jacomine PKT, Anjos LHC et al. Sistema brasileiro de classificação de  
916 solos. 3. Ed, Brasília, DF: Embrapa, 2013. 353 p.
- 917 Santos S, Ochman H. Identification and phylogenetic sorting of bacterial lineages  
918 with universally conserved genes and proteins. *Environ Microbiol* 2004; 6:754-59,  
919 DOI:10.1111/j.1462-2920.2004.00617.x.

- 920 Schlemper TR, Leite MFA, Lucheta AR. Rhizobacterial community structure  
921 differences among sorghum cultivars in different growth stages and soils.  
922 *FEMS Microbiol Ecol* 2017; 93, DOI: 10.1093/femsec/fix096.
- 923 Selbmann L, de Hoog GS, Zucconi L et al. Drought meets acid: three new genera in a  
924 dothidealean clade of extremotolerant fungi. *Stud Mycol* 2008; 61:1-20, DOI:  
925 10.3114/sim.2008.61.01.
- 926 Sharma N, Singhvi R. Effects of chemical fertilizers and pesticides on human health  
927 and environment: A review. *Int. j. Agric. Environ. Biotechnol* 2017; 10: 675-79, DOI:  
928 10.5958/2230-732X.2017.00083.3.
- 929 Silva UC, Medeiros JD, Leite LR et al. Long-Term Rock Phosphate Fertilization  
930 Impacts the Microbial Communities of Maize Rhizosphere. *Front. Microbiol.* 2017;  
931 8:1266, DOI: 10.3389/fmicb.2017.01266.
- 932 Soina VS, Mulyukin AL, Demkina EV et al. The structure of resting bacterial  
933 populations in soil and subsoil permafrost. *Astrobiology* 2004; 4:345–58, DOI:  
934 10.1089/ast.2004.4.345.
- 935 Stamatakis A. RAxML version 8: a tool for phylogenetic analysis and post-analysis of  
936 large phylogenies. *Bioinformatics* 2014; 30:1312–13,  
937 DOI:10.1093/bioinformatics/btu033.
- 938 Tabatabai M. Soil enzymes. In: Weaver RW, Angle S, Bottomley P et al. (eds.).  
939 Methods of Soil Analysis: Part 2 Microbiological and Biochemical Properties, 5.  
940 Madison, WI: SSSA Book Series, 1994; 775-34, DOI: 10.2136/sssabookser5.2.c37.
- 941 Trabelsi D, Cherni AE, Ben Zineb A et al. Fertilization of *Phaseolus vulgaris* with the  
942 Tunisian rock phosphate affects richness and structure of rhizosphere bacterial  
943 communities. *Appl Soil Ecol* 2017; 114, DOI:10.1016/j.apsoil.2016.11.014.
- 944 Vega NWO. A review on beneficial effects of rhizosphere bacteria on soil nutrient  
945 availability and plant nutrient uptake. *Rev Fac Nac Agron Medellín* 2007; 60:3621-43,  
946 DOI: 10.1007/s40011-013- 892 0297-0.

1  
2  
3  
4  
5  
6  
7  
8  
9  
10  
11  
12  
13  
14  
15  
16  
17  
18  
19  
20  
21  
22  
23  
24  
25  
26  
27  
28  
29  
30  
31  
32  
33  
34  
35  
36  
37  
38  
39  
40  
41  
42  
43  
44  
45  
46  
47  
48  
49  
50  
51  
52  
53  
54  
55  
56  
57  
58  
59  
60

947 Vold RL, Waugh JS, Klein MP et al. Measurement of spin relaxation in complex  
948 systems. *J. Chem. Phys* 1968; 48: 3831-32, DOI:10.1063/1.1669699.

949 Wang J, Zhou X, Guo K et al. Transcriptomic insight into pathogenicity-associated  
950 factors of *Conidiobolus obscurus*, an obligate aphid-pathogenic fungus belonging to  
951 Entomophthoromycota. *Pest Manag Sci* 2018; 74:1677-86, DOI: 10.1002/ps.4861.

952 Wu JR, Shien JH, Shieh HK et al. Cloning of the gene and characterization of the  
953 enzymatic properties of the monomeric alkaline phosphatase (PhoX) from *Pasteurella*  
954 *multocida* strain X-73. *FEMS Microbiol Lett* 2006; 267, 113-20, DOI:  
955 10.1111/j.1574-6968.2006.00542.x.

For Peer Review

## Figure Legends

**Figure 1.** A solution phosphorus-31 nuclear magnetic resonance (NMR) spectrum of the orthophosphate and phosphomonoester regions ( $\delta$  6.1 to 2.9 ppm) generated from a soil extract. Phosphorus species that have been identified within this region include: A – *neo*-IP6 in the 4-equatorial/2-axial conformation ( $\delta$  5.94 and 3.78 ppm), B – *D-chiro*-IP6 in the 2-equatorial/4-axial conformation ( $\delta$  5.70, 4.30, and 3.88 ppm), C – orthophosphate ( $\delta$  5.37 ppm), D – *myo*-IP6 ( $\delta$  5.05, 4.10, 3.72, and 3.62 ppm), E – *myo*-IP5 of the (1,2,4,5,6) enantiomers ( $\delta$  4.51, 4.01, 3.72, 3.42, and 3.30 ppm), F – *myo*-IP5 of the (1,3,4,5,6) enantiomer ( $\delta$  4.21, 3.62, and 3.30 ppm), G – *scyllo*-IP5 ( $\delta$  3.88, 3.33, and 3.15 ppm), H – *scyllo*-IP6 ( $\delta$  3.26 ppm), and I – a broad signal (centred around  $\delta$  4.10 ppm with a line-width of 300 Hz).

**Figure 2.** Solution phosphorus-31 nuclear magnetic resonance (NMR) spectra of the orthophosphate and phosphomonoester region ( $\delta$  6.1 to 2.9 ppm) on soil extracts from the surface layer of the long-term field experiment in Sete Lagoas, Brazil. Cropping treatments include continuous cultivation with sorghum (a) or maize (b). Fertiliser treatments include no addition of fertiliser P (Control – P0), the addition of rock phosphate at a rate of 100 kg fertiliser ha<sup>-1</sup> yr<sup>-1</sup> (RockP), or the addition of triple superphosphate at a rate of 100 kg fertiliser ha<sup>-1</sup> yr<sup>-1</sup> (TSP).

**Figure 3.** Phosphatase activity measured in soil collected from rhizospheres of maize and sorghum plants fertilized with either rock phosphate (RockP) or triple superphosphate fertilizer (TSP), compared to activity in unfertilized soil (P0). There was no significant effect of crop type upon enzyme activity. The effect size ( $\omega^2$ ) of fertilization upon phosphatase activity was greater under acidic conditions. Studentized Tukey-Kramer *post-hoc* pair-wise comparisons ( $Q$ ) of enzyme activity are shown. Box plots show the interpolated 25% and 75% quartiles with the median represented as a horizontal line. Whiskers indicate the minimum and maximum values. Enzyme activity was assessed by estimating the hydrolysis of disodium-*p*-nitrophenyl phosphate in buffered solutions.

**Figure 4.** The phylogenetic diversity (PD) - defined as the sum of branch lengths of the respective reference phylograms associated with metagenome reads - of small subunit



ribosomal RNA marker genes identified in rhizospheres of maize and sorghum grown in Cerrado soil. There was no significant effect of phosphorus fertilization upon PD. For each marker gene, results of analysis of variance and effect size estimates ( $\omega^2$ ) are given. Box plots indicate the interpolated 25% and 75% quartiles with the median represented as a horizontal line. Whiskers indicate minimum and maximum values. Where necessary, outliers are identified with open circles; in this case, whiskers are drawn from the limits of the upper and lower quartiles to data points less than 1.5-times the inter-quartile range.

**Figure 5.** Phylogenetic comparison of Archaeal species assemblages in rhizospheres of maize (green placements and data points) and sorghum (yellow placements and data points) grown in Cerrado soil. *A* – phylogenetic placement of metagenome reads with homology to the archaeal 16S rRNA gene in soils receiving rock phosphate (RockP – indicated with circular placements and data points), triple superphosphate (TSP – indicated with square placements and data points) or no phosphorus fertilization (P0 – indicated with triangle placements and data points). The most abundant organisms are identified on branch tips of the maximum-likelihood archaeal reference 16S rRNA phylogram. Placement symbol size is scaled to reflect relative abundance across the eighteen samples. *B* - ordination of archaeal 16S rRNA assemblages shown in *A*, exploiting the underlying phylogenetic nucleotide sequence structure (edge-PCA). Gene assemblages associated with maize and sorghum are separated on edge-PCA axis 2. Edges associated with large eigenvectors are shown in the associated colour-coded phylogram, corresponding to edge-PCA axis 2 colour scale. In this way, species associating more with either maize or sorghum are identified.

**Figure 6.** Abundance and phylogenetic diversity (PD; defined as the sum of branch lengths of the respective reference phylograms associated with metagenome reads) of phosphohydrolase genes in rhizosphere soil of maize and sorghum: no significant effect of phosphorus fertilization upon gene abundance or PD was observed. Only comparisons for which a significant effect of crop type was detected are shown. Length-normalized abundance (relative to the abundance of *atpD*, *gyrB* and *recA* single-copy genes, see methods section for calculation) and PD of gene ecotypes were consistently higher in sorghum rhizospheres where significant differences were identified by analysis of variance (ANOVA). For each gene, results of ANOVA and effect size estimates ( $\omega^2$ ) are given. Box plots indicate the interpolated 25% and 75%

quartiles with the median represented as a horizontal line. Whiskers indicate minimum and maximum values.

**Figure 7.** Phylogenetic comparison of alkaline phosphatase gene *phoD* ecotype assemblages in rhizospheres of maize (green placements and data points) and sorghum (yellow placements and data points) grown in Cerrado soil. **A** – phylogenetic placement of metagenome reads with homology to the *phoD* gene in soils receiving rock phosphate (RockP – indicated with circular placements and data points), triple superphosphate (TSP – indicated with square placements and data points) or no phosphorus fertilization (P0 – indicated with triangle placements and data points). The most abundant organisms are identified on branch tips of the maximum-likelihood archaeal reference 16S rRNA phylogram. Placement symbol size is scaled to reflect relative abundance across the eighteen samples. \* indicates the SWISS-PROT *phoD* accession. **B** - ordination of *phoD* assemblages shown in A, exploiting the underlying phylogenetic nucleotide sequence structure (edge-PCA). Gene assemblages associated with maize and sorghum are separated across both edge-PCA axes. Edges associated with large eigenvectors are shown in each axis-associated colour-coded phylogram and corresponding to the axis colour scales. In this way, ecotypes associating more with either maize or sorghum are identified.

**Figure 8.** Phylogenetic comparison of alkaline phosphatase *phoX* ecotype assemblages in rhizospheres of maize (green placements and data points) and sorghum (yellow placements and data points) grown in Cerrado soil. **A** – phylogenetic placement of metagenome reads with homology to reference *phoX* genes in soils receiving rock phosphate (RockP – indicated with circular placements and data points), triple superphosphate (TSP – indicated with square placements and data points) or no phosphorus fertilization (P0 – indicated with triangle placements and data points). Organisms harbouring the *phoX* genes with which ecotypes share homology are identified on branch tips of the maximum-likelihood *phoX* reference phylogram. Placement symbol size is scaled to reflect relative abundance across the eighteen samples. \* identifies *phoX* genes described by Majumdar *et al.* (2005), Wu *et al.* (2006), and Monds *et al.* (2006). **B** - ordination of *phoX* assemblages shown in A, exploiting the underlying phylogenetic nucleotide sequence structure (edge-PCA). Gene assemblages associated with maize and sorghum are separated on edge-PCA axis 1. Edges associated

with large eigenvectors are shown in the associated colour-coded phylogram, corresponding to edge-PCA axis 1 colour scale.

**Figure 9.** Phylogenetic comparison of non-specific acid phosphatase (NSAP) class A gene ecotype assemblages in rhizospheres of maize (green placements and data points) and sorghum (yellow placements and data points) grown in Cerrado soil. *A* – phylogenetic placement of metagenome reads with homology to reference NSAP class A genes in soils receiving rock phosphate (RockP – indicated with circular placements and data points), triple superphosphate (TSP – indicated with square placements and data points) or no phosphorus fertilization (P0 – indicated with triangle placements and data points). Organisms harbouring the NSAP class A genes with which ecotypes share homology are identified on branch tips of the maximum-likelihood gene reference phylogram. Placement symbol size is scaled to reflect relative abundance across the eighteen samples. \* identifies reference genes described by Gandhi and Chandra (2012). *B* - ordination of NSAP class A assemblages shown in A, exploiting the underlying phylogenetic nucleotide sequence structure (edge-PCA). Gene assemblages associated with maize and sorghum are separated on edge-PCA axis 1. Edges associated with large eigenvectors are shown in the associated colour-coded phylogram, corresponding to edge-PCA axis 1 colour scale.

**Figure 10.** Phylogenetic comparison of non-specific acid phosphatase (NSAP) class C gene ecotype assemblages in rhizospheres of maize (green placements and data points) and sorghum (yellow placements and data points) grown in Cerrado soil. *A* – phylogenetic placement of metagenome reads with homology to reference NSAP class C genes in soils receiving rock phosphate (RockP – indicated with circular placements and data points), triple superphosphate (TSP – indicated with square placements and data points) or no phosphorus fertilization (P0 – indicated with triangle placements and data points). Organisms harbouring the NSAP class A genes with which ecotypes share homology are identified on branch tips of the maximum-likelihood gene reference phylogram. Placement symbol size is scaled to reflect relative abundance across the eighteen samples. \* identifies reference genes described by Gandhi and Chandra (2012). *B* - ordination of NSAP class C assemblages shown in A, exploiting the underlying phylogenetic nucleotide sequence structure (edge-PCA). Gene assemblages associated with maize and sorghum are separated on both edge-PCA axis 1 and 2. Edges associated

with large eigenvectors are shown in the associated colour-coded phylogram, corresponding to the colour scales of edge-PCA axis 1 and 2.

**Figure 11.** Phylogenetic comparison of beta propeller phytase ( $\beta$ PPhy) gene ecotype assemblages in rhizospheres of maize (green placements and data points) and sorghum (yellow placements and data points) grown in Cerrado soil. *A* – phylogenetic placement of metagenome reads with homology to reference  $\beta$ PPhy genes in soils receiving rock phosphate (RockP – indicated with circular placements and data points), triple superphosphate (TSP – indicated with square placements and data points) or no phosphorus fertilization (P0 – indicated with triangle placements and data points). Organisms harbouring the  $\beta$ PPhy genes with which ecotypes share homology are identified on branch tips of the maximum-likelihood gene reference phylogram. Placement symbol size is scaled to reflect relative abundance across the eighteen samples. \* identifies reference genes described by Lim *et al.* (2007), \*\* identifies SWISS-PROT accessions.

**Supplementary Figure 1.** Expected mean unrooted phylogenetic diversity (PD – expressed as the sum of branch lengths occupied on the gene phylogenetic tree) of the assemblages of alkaline phosphatases *phoD* and *phoX*, non-specific acid phosphatase (NSAP) classes A and C and beta propeller phytase ( $\beta$ PPhy) genes at increasing rarefaction size (*k*) identified in maize and sorghum rhizospheres in soil receiving rock phosphate or super triplephosphate fertilizer or no phosphorus fertilization.

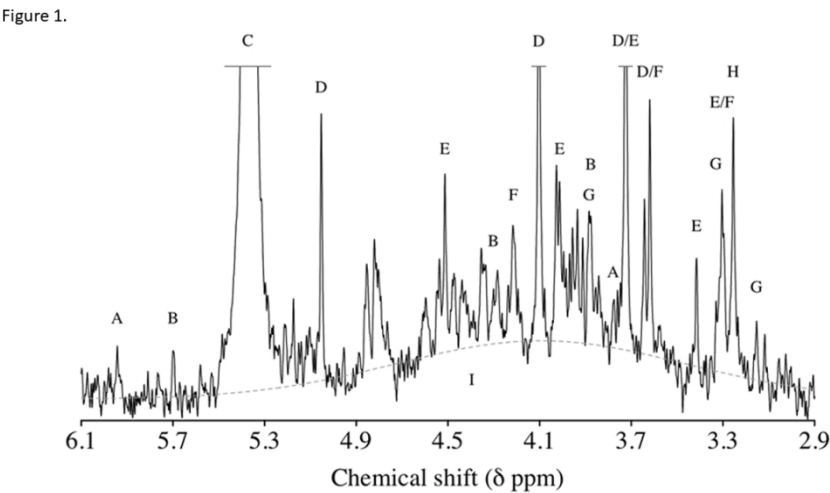


Figure 1. A solution phosphorus-31 nuclear magnetic resonance (NMR) spectrum of the orthophosphate and phosphomonoester regions ( $\delta$  6.1 to 2.9 ppm) generated from a soil extract. Phosphorus species that have been identified within this region include: A – *neo*-IP6 in the 4-equatorial/2-axial conformation ( $\delta$  5.94 and 3.78 ppm), B – *D-chiro*-IP6 in the 2-equatorial/4-axial conformation ( $\delta$  5.70, 4.30, and 3.88 ppm), C – orthophosphate ( $\delta$  5.37 ppm), D – *myo*-IP6 ( $\delta$  5.05, 4.10, 3.72, and 3.62 ppm), E – *myo*-IP5 of the (1,2,4,5,6) enantiomers ( $\delta$  4.51, 4.01, 3.72, 3.42, and 3.30 ppm), F – *myo*-IP5 of the (1,3,4,5,6) enantiomer ( $\delta$  4.21, 3.62, and 3.30 ppm), G – *scyllo*-IP5 ( $\delta$  3.88, 3.33, and 3.15 ppm), H – *scyllo*-IP6 ( $\delta$  3.26 ppm), and I – a broad signal (centred around  $\delta$  4.10 ppm with a line-width of 300 Hz).

338x190mm (96 x 96 DPI)

Figure 2.

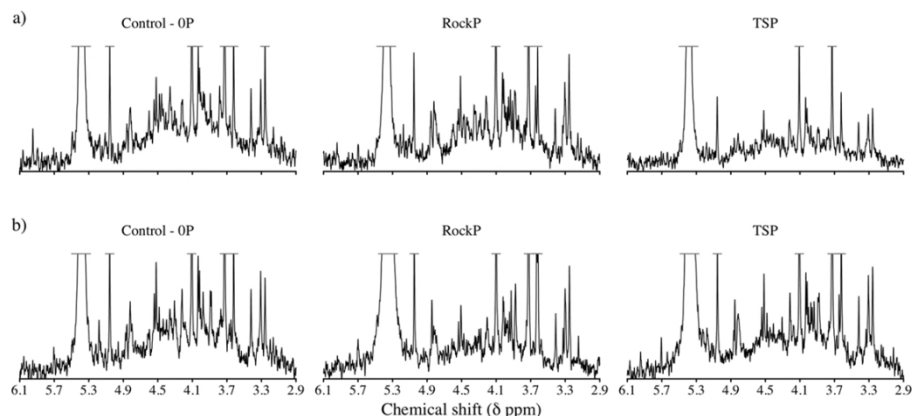


Figure 2. Solution phosphorus-31 nuclear magnetic resonance (NMR) spectra of the orthophosphate and phosphomonoester region ( $\delta$  6.1 to 2.9 ppm) on soil extracts from the surface layer of the long-term field experiment in Sete Lagoas, Brazil. Cropping treatments include continuous cultivation with sorghum (a) or maize (b). Fertiliser treatments include no addition of fertiliser P (Control – P0), the addition of rock phosphate at a rate of 100 kg fertiliser ha<sup>-1</sup> yr<sup>-1</sup> (RockP), or the addition of triple superphosphate at a rate of 100 kg fertiliser ha<sup>-1</sup> yr<sup>-1</sup> (TSP).

338x190mm (96 x 96 DPI)



Figure 3.

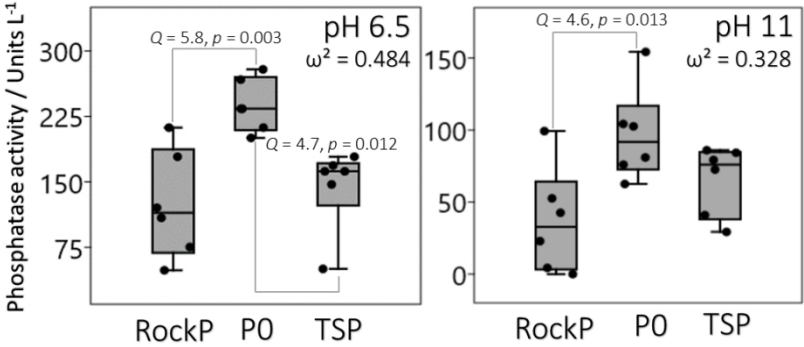


Figure 3. Phosphatase activity measured in soil collected from rhizospheres of maize and sorghum plants fertilized with either rock phosphate (RockP) or triple superphosphate fertilizer (TSP), compared to activity in unfertilized soil (PO). There was no significant effect of crop type upon enzyme activity. The effect size ( $\omega^2$ ) of fertilization upon phosphatase activity was greater under acidic conditions. Studentized Tukey-Kramer *post-hoc* pair-wise comparisons ( $Q$ ) of enzyme activity are shown. Box plots show the interpolated 25% and 75% quartiles with the median represented as a horizontal line. Whiskers indicate the minimum and maximum values. Enzyme activity was assessed by estimating the hydrolysis of disodium-p-nitrophenyl phosphate in buffered solutions.

338x190mm (96 x 96 DPI)

Figure 4.

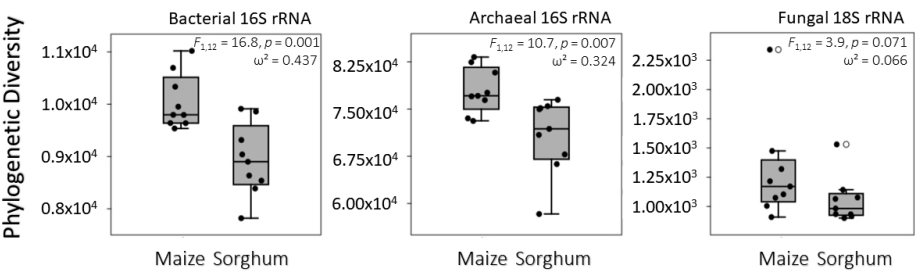


Figure 4. The phylogenetic diversity (PD) - defined as the sum of branch lengths of the respective reference phylograms associated with metagenome reads - of small subunit ribosomal RNA marker genes identified in rhizospheres of maize and sorghum grown in Cerrado soil. There was no significant effect of phosphorus fertilization upon PD. For each marker gene, results of analysis of variance and effect size estimates ( $\omega^2$ ) are given. Box plots indicate the interpolated 25% and 75% quartiles with the median represented as a horizontal line. Whiskers indicate minimum and maximum values. Where necessary, outliers are identified with open circles; in this case, whiskers are drawn from the limits of the upper and lower quartiles to data points less than 1.5-times the inter-quartile range.

338x190mm (96 x 96 DPI)

1  
2  
3  
4  
5  
6  
7  
8  
9  
10  
11  
12  
13  
14  
15  
16  
17  
18  
19  
20  
21  
22  
23  
24  
25  
26  
27  
28  
29  
30  
31  
32  
33  
34  
35  
36  
37  
38  
39  
40  
41  
42  
43  
44  
45  
46  
47  
48  
49  
50  
51  
52  
53  
54  
55  
56  
57  
58  
59  
60

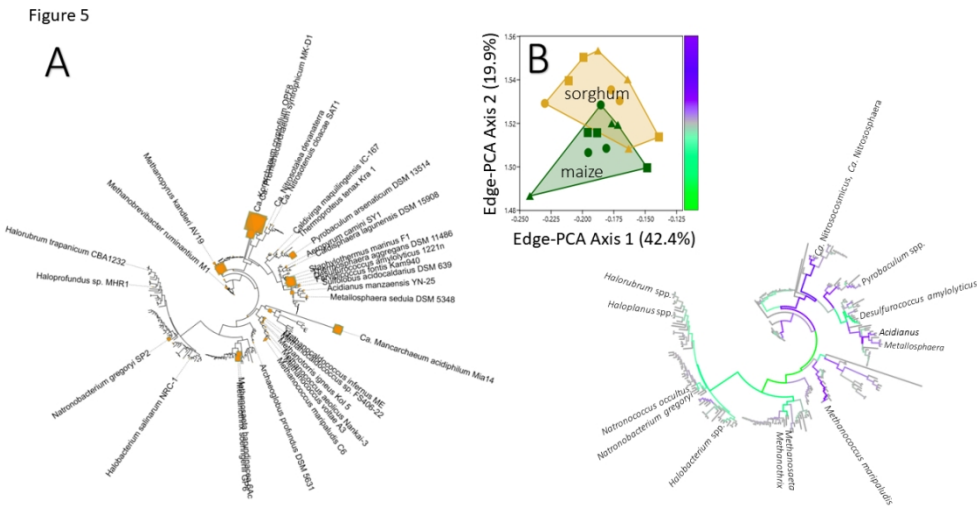


Figure 5. Phylogenetic comparison of Archaeal species assemblages in rhizospheres of maize (green placements and data points) and sorghum (yellow placements and data points) grown in Cerrado soil. A – phylogenetic placement of metagenome reads with homology to the archaeal 16S rRNA gene in soils receiving rock phosphate (RockP – indicated with circular placements and data points), triple superphosphate (TSP – indicated with square placements and data points) or no phosphorus fertilization (P0 – indicated with triangle placements and data points). The most abundant organisms are identified on branch tips of the maximum-likelihood archaeal reference 16S rRNA phylogram. Placement symbol size is scaled to reflect relative abundance across the eighteen samples. B - ordination of archaeal 16S rRNA assemblages shown in A, exploiting the underlying phylogenetic nucleotide sequence structure (edge-PCA). Gene assemblages associated with maize and sorghum are separated on edge-PCA axis 2. Edges associated with large eigenvectors are shown in the associated colour-coded phylogram, corresponding to edge-PCA axis 2 colour scale. In this way, species associating more with either maize or sorghum are identified.

338x190mm (96 x 96 DPI)

Figure 6.

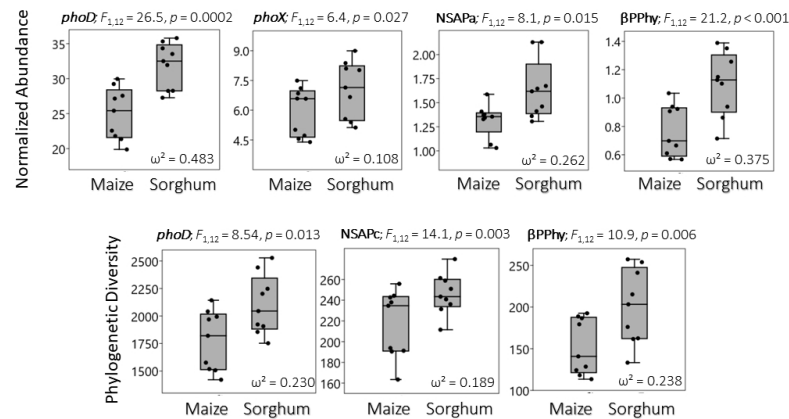


Figure 6. Abundance and phylogenetic diversity (PD; defined as the sum of branch lengths of the respective reference phylograms associated with metagenome reads) of phosphohydrolase genes in rhizosphere soil of maize and sorghum: no significant effect of phosphorus fertilization upon gene abundance or PD was observed. Only comparisons for which a significant effect of crop type was detected are shown. Length-normalized abundance (relative to the abundance of *atpD*, *gyrB* and *recA* single-copy genes, see methods section for calculation) and PD of gene ecotypes were consistently higher in sorghum rhizospheres where significant differences were identified by analysis of variance (ANOVA). For each gene, results of ANOVA and effect size estimates ( $\omega^2$ ) are given. Box plots indicate the interpolated 25% and 75% quartiles with the median represented as a horizontal line. Whiskers indicate minimum and maximum values.

338x190mm (96 x 96 DPI)

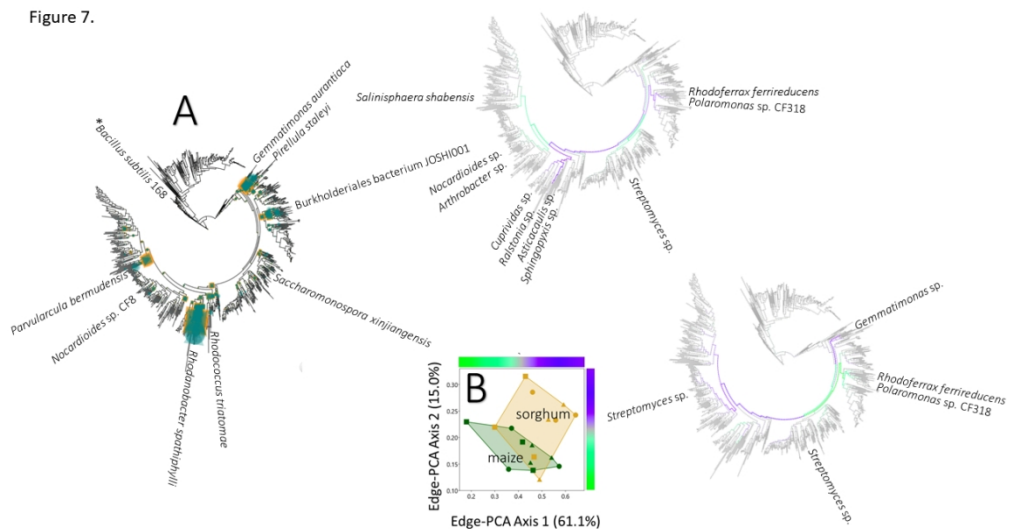


Figure 7. Phylogenetic comparison of alkaline phosphatase gene *phoD* ecotype assemblages in rhizospheres of maize (green placements and data points) and sorghum (yellow placements and data points) grown in Cerrado soil. A – phylogenetic placement of metagenome reads with homology to the *phoD* gene in soils receiving rock phosphate (RockP – indicated with circular placements and data points), triple superphosphate (TSP – indicated with square placements and data points) or no phosphorus fertilization (P0 – indicated with triangle placements and data points). The most abundant organisms are identified on branch tips of the maximum-likelihood archaeal reference 16S rRNA phylogram. Placement symbol size is scaled to reflect relative abundance across the eighteen samples. \* indicates the SWISS-PROT *phoD* accession. B - ordination of *phoD* assemblages shown in A, exploiting the underlying phylogenetic nucleotide sequence structure (edge-PCA). Gene assemblages associated with maize and sorghum are separated across both edge-PCA axes. Edges associated with large eigenvectors are shown in each axis-associated colour-coded phylogram and corresponding to the axis colour scales. In this way, ecotypes associating more with either maize or sorghum are identified.

338x190mm (96 x 96 DPI)

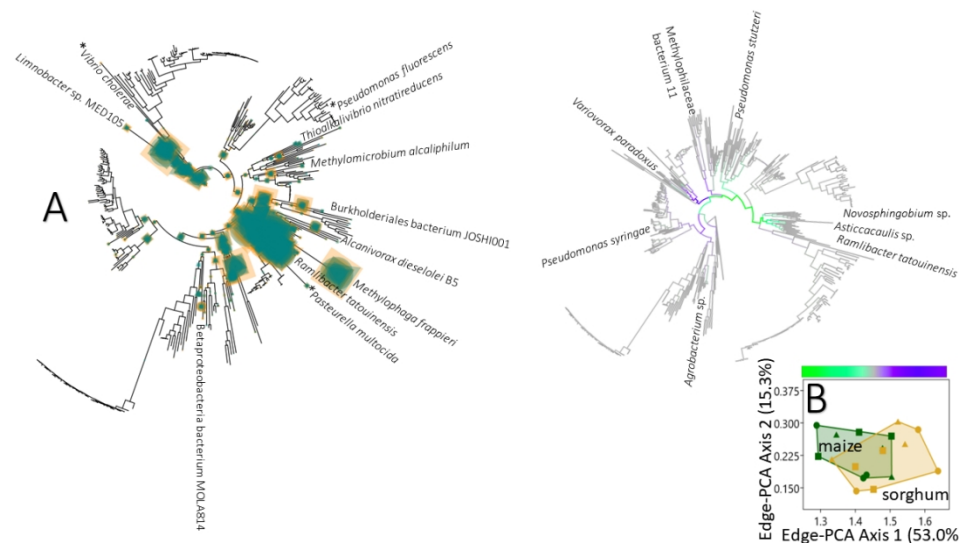
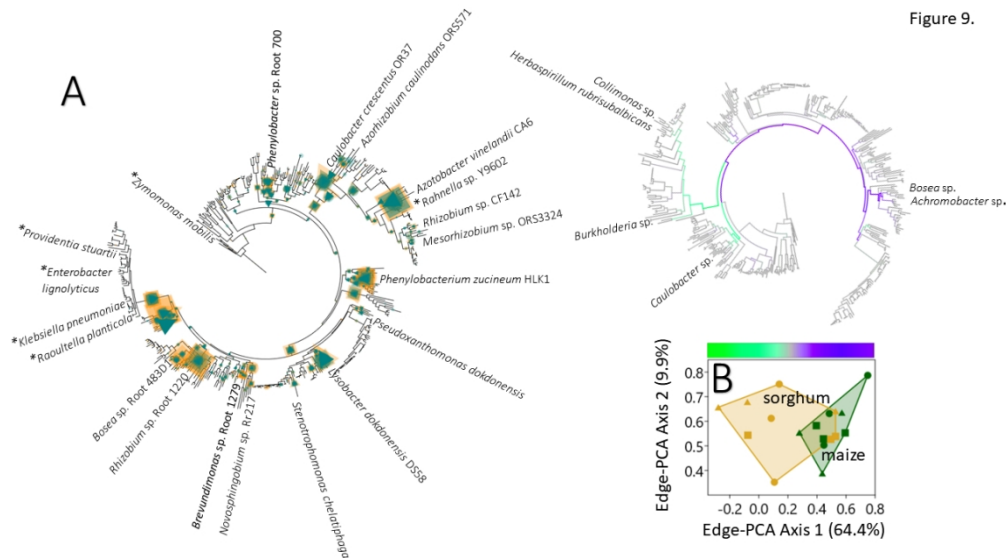


Figure 8. Phylogenetic comparison of alkaline phosphatase *phoX* ecotype assemblages in rhizospheres of maize (green placements and data points) and sorghum (yellow placements and data points) grown in Cerrado soil. A – phylogenetic placement of metagenome reads with homology to reference *phoX* genes in soils receiving rock phosphate (RockP – indicated with circular placements and data points), triple superphosphate (TSP – indicated with square placements and data points) or no phosphorus fertilization (P0 – indicated with triangle placements and data points). Organisms harbouring the *phoX* genes with which ecotypes share homology are identified on branch tips of the maximum-likelihood *phoX* reference phylogram. Placement symbol size is scaled to reflect relative abundance across the eighteen samples. \* identifies *phoX* genes described by Majumdar *et al.* (2005), Wu *et al.* (2006), and Monds *et al.* (2006). B – ordination of *phoX* assemblages shown in A, exploiting the underlying phylogenetic nucleotide sequence structure (edge-PCA). Gene assemblages associated with maize and sorghum are separated on edge-PCA axis 1. Edges associated with large eigenvectors are shown in the associated colour-coded phylogram, corresponding to edge-PCA axis 1 colour scale.

338x190mm (96 x 96 DPI)





338x190mm (96 x 96 DPI)

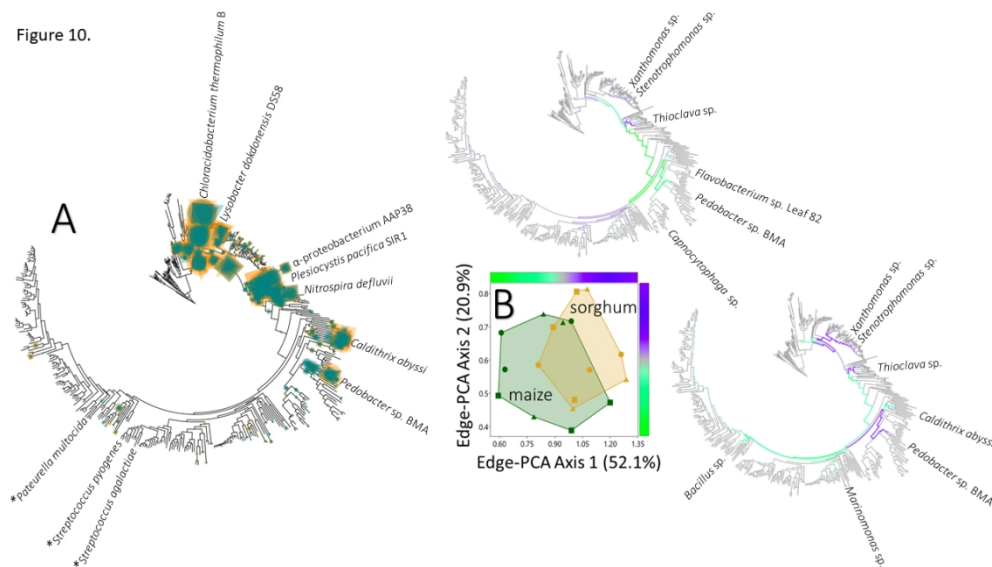


Figure 10. Phylogenetic comparison of non-specific acid phosphatase (NSAP) class C gene ecotype assemblages in rhizospheres of maize (green placements and data points) and sorghum (yellow placements and data points) grown in Cerrado soil. A – phylogenetic placement of metagenome reads with homology to reference NSAP class C genes in soils receiving rock phosphate (RockP – indicated with circular placements and data points), triple superphosphate (TSP – indicated with square placements and data points) or no phosphorus fertilization (P0 – indicated with triangle placements and data points). Organisms harbouring the NSAP class A genes with which ecotypes share homology are identified on branch tips of the maximum-likelihood gene reference phylogram. Placement symbol size is scaled to reflect relative abundance across the eighteen samples. \* identifies reference genes described by Gandhi and Chandra (2012). B - ordination of NSAP class C assemblages shown in A, exploiting the underlying phylogenetic nucleotide sequence structure (edge-PCA). Gene assemblages associated with maize and sorghum are separated on both edge-PCA axis 1 and 2. Edges associated with large eigenvectors are shown in the associated colour-coded phylogram, corresponding to the colour scales of edge-PCA axis 1 and 2.

338x190mm (96 x 96 DPI)

Figure 11.

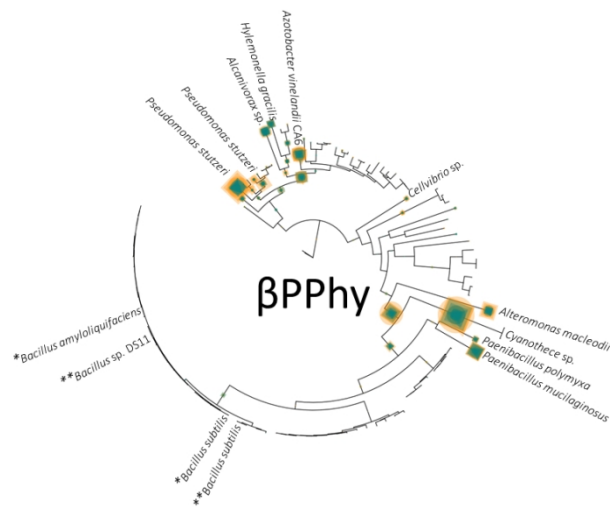


Figure 11. Phylogenetic comparison of beta propeller phytase (βPPhy) gene ecotype assemblages in rhizospheres of maize (green placements and data points) and sorghum (yellow placements and data points) grown in Cerrado soil. A – phylogenetic placement of metagenome reads with homology to reference βPPhy genes in soils receiving rock phosphate (RockP – indicated with circular placements and data points), triple superphosphate (TSP – indicated with square placements and data points) or no phosphorus fertilization (P0 – indicated with triangle placements and data points). Organisms harbouring the βPPhy genes with which ecotypes share homology are identified on branch tips of the maximum-likelihood gene reference phylogram. Placement symbol size is scaled to reflect relative abundance across the eighteen samples. \* identifies reference genes described by Lim et al. (2007), \*\* identifies SWISS-PROT accessions.

338x190mm (96 x 96 DPI)

**Table 1.** Concentrations (mg kg<sup>-1</sup>) of phosphorus (P) species in NaOH-EDTA extracts of one replicate of the three fertiliser treatments under continuous cropping from sorghum or maize as determined from solution <sup>31</sup>P nuclear magnetic resonance (NMR) spectroscopy. Rock phosphorus (RockP) and triple superphosphate (TSP) treatments were associated with the addition of 100 kg of fertiliser ha<sup>-1</sup> yr<sup>-1</sup>. No phosphorus was added to the control treatment (P0).

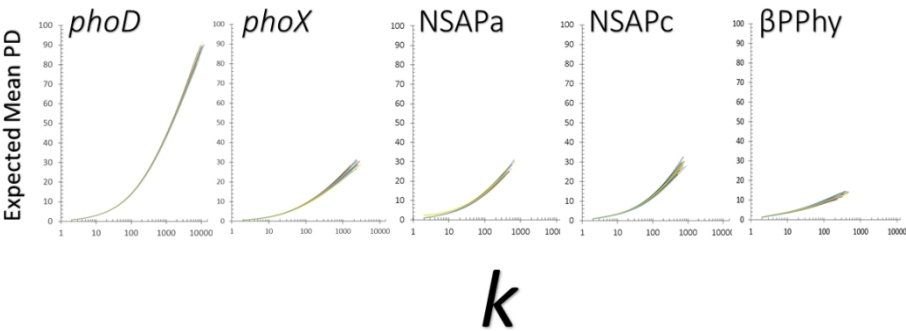
P species	Sorghum			Maize		
	P0	RockP	TSP	P0	RockP	TSP
Phosphonates						
2-AEP	0.0	0.6	0.7	0.5	0.0	0.6
Other <sup>a</sup>	0.0	0.0	0.0	0.0	0.0	0.4
Orthophosphate	159.5	174.6	274.6	219.6	463.2	344.7
Phosphomonoester						
Broad signal	54.3	34.1	63.2	55.3	37.0	55.1
<i>myo</i> -IP6	19.0	16.5	17.9	16.8	19.5	20.9
<i>scyllo</i> -IP6	3.4	2.1	1.9	1.5	2.0	2.0
<i>neo</i> -IP6	1.5	0.7	0.0	0.0	0.0	0.0
D- <i>chiro</i> -IP6	0.0	1.6	0.0	1.5	2.6	2.1
<i>myo</i> -IP5 <sup>b</sup>	6.6	8.5	9.9	8.0	7.2	9.7
<i>scyllo</i> -IP5	1.7	1.8	0.0	0.8	1.0	1.2
<i>scyllo</i> -IP4	0.8	0.0	0.0	0.5	0.0	0.0
Other <sup>a</sup>	16.2	20.5	9.9	9.0	11.7	10.3
Phosphodiester						
DNA	5.6	0.0	4.8	3.6	0.0	0.0
Other <sup>a</sup>	0.5	0.0	0.0	0.0	0.0	0.0
Polyphosphate						
	8.0	3.0	7.6	3.9	2.6	2.8

Pyrophosphate						
Other <sup>a</sup>	0.0	0.0	0.0	0.3	0.0	0.0
Total P	276.9	263.9	390.6	321.3	547.2	449.8
Inorganic P	167.5	177.6	282.2	223.8	465.8	347.5
Organic P	109.4	86.3	108.3	97.5	81.4	102.3

<sup>a</sup> Summation of all sharp signals of unknown identity within the phosphonate, phosphomonoester, phosphodiester or polyphosphate regions.

<sup>b</sup> Summation of *myo*-IP5 of the (1,2,4,5,6) and (1,3,4,5,6) enantiomers.

Supplementary Figure 1.



338x190mm (96 x 96 DPI)